Implementation of Small Diameter Borehole Thermal Experiments at WIPP

Spent Fuel and Waste Disposition

Prepared for
U.S. Department of Energy
Used Fuel Disposition Campaign
DOE Milestone M3SF-18LA010303014

H. Boukhalfa, P.J. Johnson, D. Ware, D.J. Weaver, S. Otto,
B.L. Dozier, P.H. Stauffer
Los Alamos National Laboratory

M.M. Mills, E.N. Matteo, N.B. Nemer, C.G. Herrick, K.L. Kuhlman
Sandia National Laboratories

Y. Wu, J. Rutqvist
Lawrence Berkeley National Laboratory

September 24, 2018

LA-UR-18-29203

FCT Quality Assurance Program Document

Appendix E
FCT Document Cover Sheet

Name/Title of Deliverable/Milestone	**Implementation of a Small Borehole Heater Test at WIPP**
Work Package Title and Number	**SF-18LA01030301 Salt R&D - LANL**
Work Package WBS Number	1.08.01.03.03 - Salt Disposal R&D
Responsible Work Package Manager	Philip H. Stauffer [signature] (Name/Signature)
Date Submitted	

Quality Rigor Level for Deliverable/Milestone	☒ QRL-3	☐ QRL-2	☐ QRL-1 ☐ Nuclear Data	☐ N/A*

This deliverable was prepared in accordance with Los Alamos National Laboratory
(Participant/National Laboratory Name)

QA program which meets the requirements of
☒ DOE Order 414.1 ☐ NQA-1-2000

This Deliverable was subjected to:

☐ Technical Review	☐ Peer Review
Technical Review (TR)	**Peer Review (PR)**
Review Documentation Provided	**Review Documentation Provided**
☐ Signed TR Report or,	☐ Signed PR Report or,
☐ Signed TR Concurrence Sheet or,	☐ Signed PR Concurrence Sheet or,
☒ Signature of TR Reviewer(s) below	☐ Signature of PR Reviewer(s) below

Name and Signature of Reviewers
Robert Roback [signature] 9-26-18

*Note: In some cases there may be a milestone where an item is being fabricated, maintenance is being performed on a facility, or a document is being issued through a formal document control process where it specifically calls out a formal review of the document. In these cases, documentation (e.g., inspection report, maintenance request, work planning package documentation or the documented review of the issued document through the document control process) of the completion of the activity along with the Document Cover Sheet is sufficient to demonstrate achieving the milestone. QRL for such milestones may be also be marked N/A in the work package provided the work package clearly specifies the requirement to use the Document Cover Sheet and provide supporting documentation.

REVISION HISTORY

Revision Number	Effective Date	Pages Revised	Description of Revision
0		N/A	Initial Issue

Table of Contents

1. Summary 1

2. Introduction 1
   2.1. Safety Case for Disposal of Heat Generating Nuclear Waste in Salt 2
   2.2. Need of Field-Testing Campaign 3
   2.3. Small Borehole Test Design 4
   2.4. Technical Objectives 5

3. Experimental Methods and Procedures 5
   3.1. Work Plan 5
   3.2. Training and Authorization to Work in the Underground at WIPP 6
   3.3. Existing Underground Boreholes at WIPP and Testing Availability 8
   3.4. Phase 1 Test Configuration 11
   3.5. Design of Phase 1 Heater Assembly 12
   3.6. Design of Phase 1 Borehole Deformation Gage 16
   3.7. Design of Phase 1 Packer Assembly and Instrumentation 19
   3.8. Design of Phase 1 Moisture Collection and Permeability Measurement System 19
   3.9. Design of Phase 1 Brine Collection System 21
   3.10. Design of Phase 1 ERT System 22
   3.11. Phase 1 Data Logging 24

4. Phase 1 Testing Summary 24
   4.1. Phase 1 Gas Permeability Measurements. 24
   4.2. Phase 1 Moisture Collection and Brine Inflow Measurements 26
   4.3. Phase 1 Heater Controlled to a Set Point Temperature 30

5. Simulations of the Phase 1 Thermal Test 35
   5.1. Simulation details 35
   5.2. Simulations of Phase 1 Pressure Decay. 38
   5.3. Simulations of Phase 1 Moisture Removal 39
   5.4. Simulations of Phase 1 Temperature Changes 41

6. Conclusions and Recommendations 43

7. References 44

8. Appendix A: Components Design and Specifications 46
   8.1. Heating Element Specifications 47
   8.2. Heating Block Specifications 48
   8.3. Temperature Controller 49
   8.4. Packer Assembly Specifications 50
   8.5. Borehole Deformation Gauge Specification 54
   8.6. Brine Inflow Measurements 56
   8.7. Data Acquisition and Logging 60

9. Appendix B: Working Underground at WIPP 60
   9.1. Qualifications and Training 60

9.2. Health and Safety 61
9.3. Permits and Authorizations 61

LIST OF TABLES

Table 1. Summary of boreholes used in the Phase 1 testing. 10

Table 2. Summary of RTDs and thermocouples deployed in and around the heater 15

Table 3. Material properties of the simulations 37

LIST OF FIGURES

Figure 1. Location of the existing boreholes used in Phase 1 testing. 9

Figure 2. Configuration of existing boreholes used in Phase 1 testing. SNLCH111 is the right most 12 cm boreholes and numbering increases to the left. 10

Figure 3. Schematic cross-section view of the borehole and instrumentation in Phase 1 heater test. 11

Figure 4. Photograph showing the heater assembly being laboratory tested in Run-of-Mine salt 12

Figure 5. Temperature data showing drop off in temperature in the Run-of-Mine salt away from the heater. 13

Figure 6. Picture of the Phase 1 LVDT device constructed to measure borehole closure 18

Figure 7. Pre-assembly test of Phase 1 packer system used to isolate the heated borehole from the access drift. 19

Figure 8. Simplified diagram showing the Phase 1 moisture collection and gas permeability measurement systems. 20

Figure 9. As-built rendering of Phase 1 heater/packer assembly. 21

Figure 10. The Phase 1 heater/packer assembly prior to installation. 22

Figure 11. Schematic cross-section of the Phase 1 ERT data acquisition layout. 23

Figure 12. Schematic diagram showing the Phase 1 setup used for gas permeability measurements. 25

Figure 13. Experimental data results showing the pressure decay recorded during Phase 1 permeability testing. 26

Figure 14. Plot showing water extraction by nitrogen circulation through the isolated interval of the borehole (Phase 1). 28

Figure 15. Plot of the total moisture captured by the desiccant cartridges as a function of observation days (Phase 1). 29

Figure 16. Schematic representation of the positions of the Phase 1 temperature probes. 30

Figure 17. Schematic representation of the layout of the different boreholes instrumented in Phase 1 testing. 31

Figure 18. Phase 1 temperature profiles recorded by thermocouples and RTDs during the heater test in the heated packer borehole. The different colored lines represent individual thermocouples and RTDs positioned at different distances from the heater. 32

Figure 19. Temperature profiles recorded by thermocouples and RTDs during the heater test in the temperature borehole. The different colored lines represent individual thermocouples and RTDs positioned at different distances from the heater. 34

Figure 20 Temperature profiles recorded by thermocouples and RTDs during the heater test in the small temperature borehole. The locations of the temperature probes are shown in Figure 16...35

Figure 21. Drift face view of the numerical mesh showing the borehole as red with the rock salt as dark blue. 36

Figure 22. Side view of the numerical mesh showing the borehole as red with the packer interval as green and the heater as light blue. Rock salt is dark blue. 37

Figure 23. Phase 1 experimental pressure decay compared to simulation results. 39

Figure 24. Water mass removal through the nitrogen flow system, Phase 1 data vs simulations. 40

Figure 25 Temperature as a function of time at TB0 and TSB0, model vs data 41

Figure 26. Fully coupled heater simulation. 42

Figure 27 MIN coupled heater block 43

ACRONYMS

AE	Acoustic emission
CBFO	Carlsbad Field Office
CRDS	Cavity ring-down spectrometer
DOE	Department of Energy
DOE-EM	Department of Energy Office of Environmental Management
DOE-NE	Department of Energy Office of Nuclear Energy
DRZ	Disturbed rock zone
EDZ	Excavation damage zone
ERT	Electric resistivity tomography
ISMS	Integrated safety management system
LANL	Los Alamos National Laboratory
LANL-CO	Los Alamos National Laboratory – Carlsbad Operations
LBNL	Lawrence Berkeley National Lab
LVDT	Linear variable differential transformer
M&O	Management & Operations
M&TE	Measuring and test equipment
NWP	Nuclear Waste Partnership LLC (WIPP M&O contractor)
PI	Principal investigator
QA	Quality assurance
ROM	Run-of-mine salt
RTD	Resistive temperature device
SDI	Salt disposal investigations
SDDI	Salt defense disposal investigations
SEM	Scanning electron microscope
SNL	Sandia National Laboratories
TCO	Test Coordination Office
WIPP	Waste Isolation Pilot Plant

1. Summary

This report summarizes initial work done in a phased thermal testing program in bedded salt at the Waste Isolation Pilot Plant (WIPP), Carlsbad, New Mexico. The testing to date has been focused on existing boreholes and is being used to 'shakedown' the process for implementation in freshly drilled boreholes planned for FY2019. The report begins with a brief introduction to the problem including technical objectives of the testing program (Section 2). Next, we review the experimental methods and procedures that were used (Section 3. Section 4 summarizes the measurements that have been made to date, while Section 5 describes preliminary numerical analysis that has revealed useful information about system behavior. A brief conclusions section includes some recommendations that we generated through field observations and numerical analysis. Appendix A contains specifications on individual components of the experiment, while Appendix B provides copies of necessary training and permit documents needed to perform the experiment in the underground at WIPP.

2. Introduction

Safe and permanent isolation of spent nuclear fuel and high-level nuclear waste (HLW) is an integral component of radioactive waste management. Rock types considered for the permanent deep disposal of nuclear waste, include: tuff, shale, granite, clay, and salt. Recent work in the US has focused on studying generic salt reposory concepts [**1-4**]. Historically, disposal in salt has received significant interest and was investigated through several testing campaigns in the U.S. and in Germany [**5-11**]. The disposal of nuclear waste in salt is particularly appealing because of the availability of salt formations that can accommodate the design and construction of repositories and the advantage offered by salt as an impermeable and dry medium with self-sealing properties [**12**]. This report presents a short summary of some of the knowledge gaps identified in our state of knowledge assessment that are relevant to strengthening the safety case for the disposal of heat generating waste in salt, and the development of a focused field-testing campaign to study brine generation in heated salt.

2.1. Safety Case for Disposal of Heat Generating Nuclear Waste in Salt

Considerations of using salt formations for the disposal of heat generating nuclear waste (HGNW) have had support of the scientific community since early 1950s. Salt formations in the U.S. exist over large geographic areas [**13**]. Bedded salt formations with thicknesses often between 200 to 600 meters present favorable geologic settings for the construction of nuclear waste repositories. Extensive *in situ* field testing in salt was performed in the U.S. and abroad to evaluate the performance of salt as a medium for the disposal of nuclear waste. Studies in bedded salt near Lyons, Kansas in 1965 were carried out to examine the effects of HLW in bedded SALT [**5**]. Studies were also performed from 1967-1978 [**14**] in the Asse salt mine to evaluate the behavior of salt in the presence of elevated-temperature HLW (**6**). Testing was performed at the Avery Island salt mine in 1979 in Louisiana to examine brine migration and generation resulting from heating. Experimentation with heat generating elements was also carried out at the WIPP facility in New Mexico during the 1980s and early 1990s [**10**]. A report summarizing previous testing efforts was recently complied [**15**]. A field testing effort was designed by DOE-EM to address some of the knowledge gaps identified from the review of the historical data and explore a new disposal concept (SDI and SDDI). These drift-scale disposal demonstrations were not implemented because DOE-NE sought an effort that builds on experimentation and an intermediate scale is necessary before any large testing effort is performed. To this end, an intermediate scale testing effort was started to regain hands-on experience by performing in situ testing at WIPP and to address some of the knowledge gaps at a manageable scale. The intermediate testing campaign was developed in the previous years and the test design was published in a consensus document that outlined the goals and approach of performing the test [**16**].

2.2. Need of Field-Testing Campaign

Better understanding of the source, chemical composition, and fate of brine produced from heated bedded salt (i.e., brine availability) contributes to our ability to accurately predict the long-term performance of salt as a medium for the permanent isolation of nuclear waste [**16,17**]. Brine availability is relevant to three aspects of the waste isolation safety case: (1) water-driven corrosion of the metal waste packages and waste forms; (2) moisture-enhanced closure of excavations and brine backpressure effects on excavation closure; and (3) short-term drift-scale brine redistribution processes. Past examinations in the laboratory and in the field have shown that gas-free fluid inclusions migrate toward a heat source, brine moves under a pressure gradient near an excavation, and that evaporation and condensation of vapor changes the porosity of the salt near the heat source. However, modeling efforts would be improved by validation dataset regarding the quantity and composition of the brine that is likely to come in contact with the waste packages. Numerical models have been developed to couple the thermal properties of waste packages to the behavior of salt and brine availability in salt. There is a need to collect more experimental data on brine availability from the far field, and to collect datasets that can be used to validate and improve numerical models, which can be used to enhance long-term repository performance predictions. Run-of-Mine (ROM) salt reconsolidation is affected by the amount of available brine [**17,18**], with small amounts of brine enhancing reconsolidation significantly. The intermediate scale testing effort described in this document was developed with the goal of answering some of the questions related to brine availability and migration. Additionally, the intermediate heater test is developed to test instrumentation and new analysis approaches for brine and gas sample collection, characterization of the enhanced permeability and porosity surrounding a borehole, and the effects temperature have on these processes in bedded salt.

2.3. Small Borehole Test Design

The proposed intermediate heater test campaign planned is staged in two phases. The first phase (Phase 1) of testing utilizes four existing 4.75” sub-horizontal boreholes and focuses on equipment/methods development, personnel training, confidence building, and construction deployment of a heater/packer assembly underground at WIPP. The first phase includes periods of up to 3 weeks of testing at ambient temperature to collect baseline data followed by over 3 weeks of a heated experiment with the heater assembly at a set point of 120 ^{o}C. Following a cool down that is planned to last through September 28, 2018, the first phase is poised to implement heating in steps to test the system at higher temperatures and also test gas collection for analytical chemistry. The preliminary data from this test will be used to inform our implementation of the second phase. The second phase of testing (Phase 2) will be conducted in newly-drilled sub-horizontal boreholes that will be freshly drilled to conduct the planned testing. A revised experimental design will be developed based on the test plan developed previously [**17**] and lessons learned from the first phase of testing.

An assembly of heater and packer was installed in an existing 4.75" borehole with supporting instruments installed in both the heated borehole and in adjacent boreholes. Temperature of the heater and borehole near the heater were monitored continually through alternating ambient and heated periods. Brine inflow to the heated borehole was also estimated gravimetrically by a downstream moisture collection system. Liquid brine samples that accumulated in the borehole before the start of the heating were analyzed in the laboratory for composition. Borehole diameter was monitored to observe borehole closure using an LVDT-based centralizer system emplaced in the borehole between the packer and the heater assembly. Changes in the sealing capability of the packer and near-borehole formation was also characterized by pressurizing the borehole interval behind the packer and observing transient pressure decay. The packer/heater design, deployment and preliminary data will be presented in this report.

2.4. Technical Objectives

The technical details and goals of the intermediate heater test were laid out initially in previous report [**19**] and further refined in a consensus document as a joint LANL-CO, LBNL, SNL, and LANL effort [**16**]. This test plan is developed in accordance with Phase 1 of consensus test plan described in reference [**16**]. Section 1.1 of that document laid out four goals:

1) Constrain brine availability and brine chemistry in bedded salt;
2) Collect datasets that can be used to validate numerical models and improve understanding of the constitutive and conceptual models applied to generic salt repository science;
3) Collect field data to improve understanding of acid gas generation mechanisms; and
4) Maintain the legacy of underground tests at WIPP and ensure continuity of knowledge and experience.

3. Experimental Methods and Procedures

3.1. Work Plan

The work plan developed is based on a phased approach that will advance the design of the heater packer and instrumentation and incorporate the lessons learned from early testing to better achieve the technical objectives of the intermediate borehole heater test described above. The work plan also must meet the safety regulations and requirements for working underground at WIPP. Feedback through the initial prototyping studies and lessons learned from performing experiments at the underground at WIPP will be incorporated in the design and implementation of the heater test planned in Phase 2. The following tasks were executed in Phase 1:

1. Training and authorization to work in the underground at WIPP.
2. Characterization of existing borehole underground at WIPP and their availability for testing.
3. Design of a packer/heater assembly and instrumentation fielded in Phase 1 testing
    a. Phase 1 test configuration
    b. Design procurement and installation of instrumentation in support of the heater test
    c. Construction of a moisture collection assembly
    d. Design and construction of an LVDT system
4. Experimental testing
    a. Design of a permeability testing procedure
    b. Initial testing under isothermal conditions
    c. Initial heating
5. Lessons learned

Each task is described in more details in the following sections.

3.2. Training and Authorization to Work in the Underground at WIPP

The Waste Isolation Pilot Plant (WIPP) is principally designed and operated as a deep geologic repository for permanent isolation of long-lived radioactive waste. It is also host to a number of experiments that take advantage of the unique environmental characteristics found in an underground salt formation, such as the absence or minimization of naturally occurring radioactive elements, and shielding from cosmic rays by the overlying rock. In addition, the WIPP provides a platform for field-scale and borehole tests of salt repository performance for waste forms other than the transuranic (TRU) waste for which it is currently authorized.

Due to the size, duration, and complexity of the science and testing activities in the WIPP underground, the DOE Carlsbad Field Office established the WIPP underground Test Coordination Office (TCO) in early 2013 to ensure that underground science activities are coordinated, implemented, and managed in an integrated, consistent, efficient, cost-effective, safe, and environmentally compliant manner. The TCO also helps to ensure, through rigorous planning, scheduling, consistent site-interface, and work requests that the science activities are supported with WIPP infrastructure, but in a manner as not to interfere with the WIPP's primary mission, the disposal of transuranic (TRU) waste.

Performing work underground at WIPP requires close integration and planning with TCO, through which training, scheduling, work control, work authorization, work release, site infrastructure, and site access is organized. The hazards associated with this work are principally chemical, electrical, environmental, and thermal. The health and safety hazards are controlled and mitigated through TCO Work Control Documents and associated Job Hazard Analyses developed in accordance with TCO site-specific procedures. Work Control Documents provide detailed work definition, hazard analysis, and hazard controls, developed using an iterative process involving the TCO, the principle investigators, works, and the WIPP M&O contractor. The work is reviewed, scheduled, authorized, and released through formal process with the WIPP M&O contractor ad is overseen by the TCO and other organizations to ensure compliance. All personnel who conduct work activities underground at WIPP are required to pass, at a minimum, the WIPP General Employee and Underground Hazard training. Pre-job briefings were conducted for the specific work activities before the start of operations and an assessment was conducted at the conclusion of the work to establish lessons learned. These lessons learned are being used to help design and implement the next phase of testing.

3.3. Existing Underground Boreholes at WIPP and Testing Availability

Phase 1 testing was performed in existing bore holes drilled in 2012 in the E-140 drift between N-940 and N-1100 (**Figure 1**). Prior to the initial testing each one of the existing boreholes was video logged and samples of brine and salt precipitant were collected from inside the boreholes for analysis. **Table *1*** summarizes the characteristics of each borehole. **Figure *2*** shows a picture of the wall of the E-140 drift on which the existing horizontal boreholes are located. Also seen in this picture are the rock bolts and chain link fence used to secure the drift face (i.e., ground control). The image predates the installation of the bulk of the experiment; however the power supply junction boxes can be seen to the right of the existing boreholes.

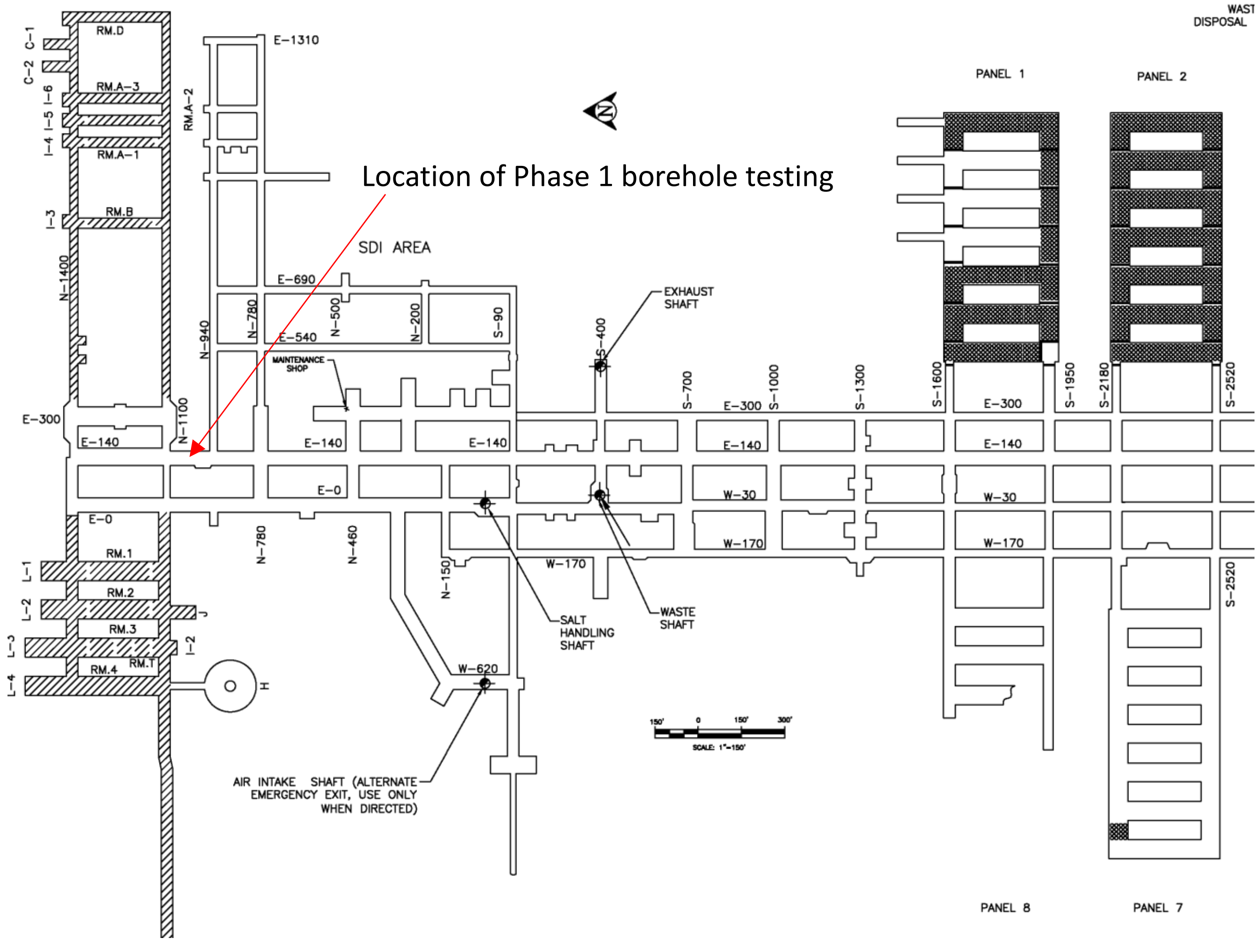

Figure 1. Location of the existing boreholes used in Phase 1 testing.

Table 1. Summary of boreholes used in the Phase 1 testing.

Borehole ID	Approximate diameter, Centimeters	Approximate depth, meters	Approximate distance between boreholes in cm	Comments
SNLCH111	12	4.4		Large amount of pooled brine at end of borehole
SNLCH112	12	5.49	48.76 cm between SNLCH112 and SNLCH111	Large amount of pooled brine at end of borehole
SNLCH113	12	6.05	32 cm between SNLCH113 and SNLCH112	Large amount of pooled brine at end of borehole
SNLCH114	12	6	30 cm between SNLCH114 and SNLCH113	Large amount of pooled brine at end of borehole
no id/ little borehole	3.35	3.96	23 cm between SNLCH112 and small borehole	Large amount of pooled brine at end of borehole

Figure 2. Configuration of existing boreholes used in Phase 1 testing. SNLCH111 is the right most 12 cm boreholes and numbering increases to the left.

3.4. Phase 1 Test Configuration

The design and experiments performed in Phase 1 and described in the current document was detailed in our previous reports Kuhlman et al. (2017) and illustrated in ***Figure 3***.

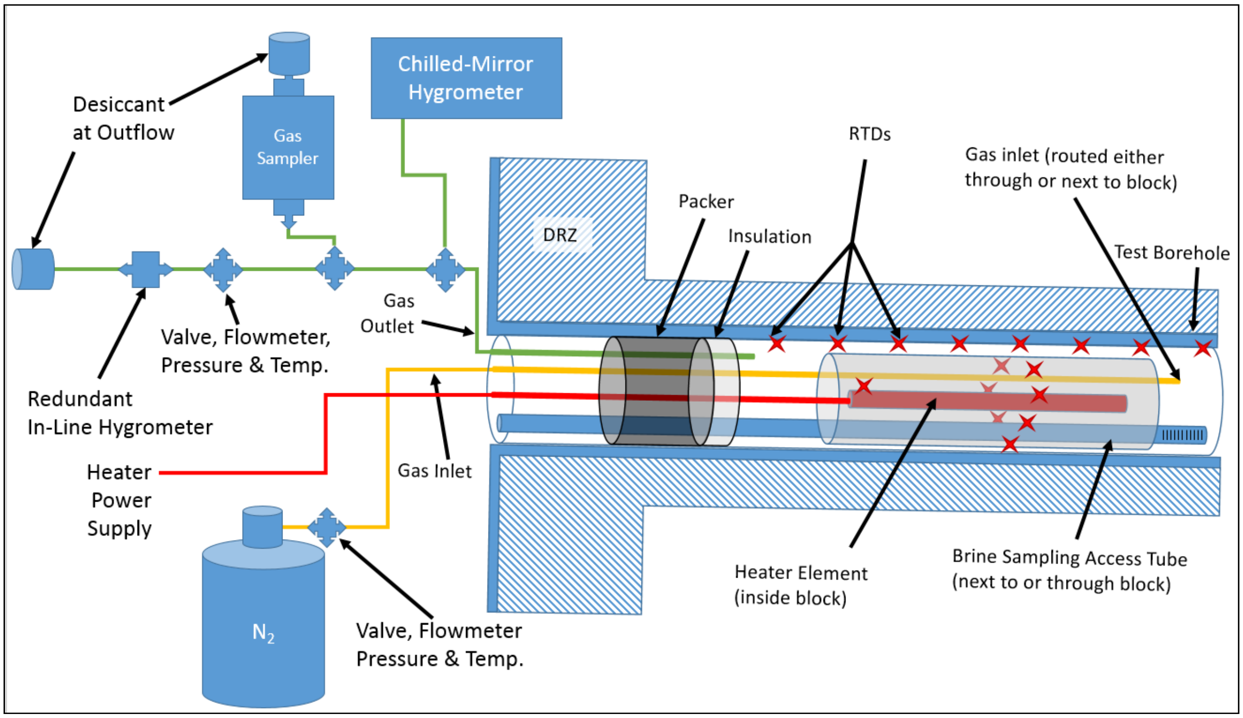

Figure 3. Schematic cross-section view of the borehole and instrumentation in Phase 1 heater test.

The main components of the system deployed and tested in Phase 1 include: a packer system designed to isolate the heated portion of the borehole from the access drift, a heater embedded in a steel block, an array of thermocouples along the heater block, access tube to allow access to the back of the borehole brine collection, and a nitrogen flow moisture accumulation system to quantify the removal moisture from the borehole behind the packer, to quantify brine inflow into the borehole. The heater/packer assembly and accompanying instrumentation were assembled into a connected train. The components of the assembly were mounted around a one-inch diameter steel pipe through which wires from the heater, thermocouples, RTDs, and LVDT passed to the access drift. The void space between the wires and the pipe was filled with an epoxy resin to seal the pipe.

3.5. Design of Phase 1 Heater Assembly

The heater assembly used in Phase 1 testing consisted of a stainless steel heater block heated by a Watlow heater cartridge. This assembly was developed in our laboratory testing phase and was extensively tested in a 2 ft × 2 ft × 2 ft Plexiglas box filled by Run-off-Mine salt. A picture of the heater assembly imbedded in Run-of-Mine salt for laboratory testing is shown in **Figure *4***. The temperature of the stainless steel block during heating was fixed to a set point by a temperature controller.

Figure 4. Photograph showing the heater assembly being laboratory tested in Run-of-Mine salt

Heating of the steel block happens quickly and temperature control to a set point is very effective. However, we found that there is poor coupling between the steel heating block and salt, which results in up to 100°C difference between the temperature at the surface of the heater and the salt close to the heater. This poor coupling between the salt and the heater is likely to be an important parameter to consider for the borehole heater test design. Reaching the target maximum temperatures of 50°C, 120°C, 160°C, and 200°C might require adjusting the heater block assembly to tens of degrees higher than the target maximum temperatures. ***Figure 5*** shows an example of the data obtained during the laboratory heater testing.

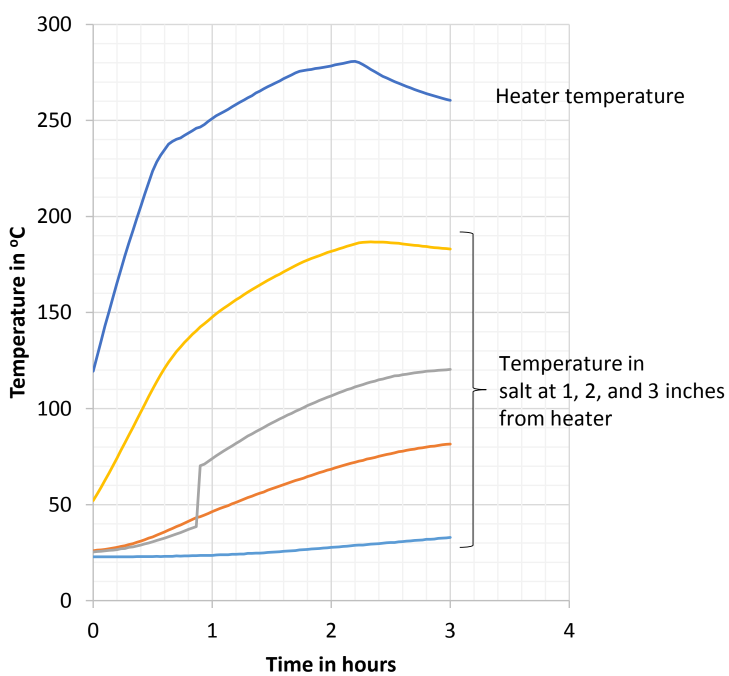

Figure 5. Temperature data showing drop off in temperature in the Run-of-Mine salt away from the heater.

The final design of the heater assembly was modified slightly to accommodate mounting the heater in the delivery train assembly deployed in the borehole. The technical details of the heater components and actual pictures of the assembly are provided in Appendix 1.

Thermocouples/RTDs locations

Thermocouples and RTDs were used to measure the temperature in the borehole and around the heater. The thermocouples were also deployed to measure the temperature in parallel boreholes located a few inches below the heated borehole. The location of the thermocouples and RTDs and their description are summarized in ***Table 2***.

Table 2. Summary of RTDs and thermocouples deployed in and around the heater

Wire Number	Description	Model	Temp Rating, deg C	DAS Name Notes	Distance from Top of Borehole, in	Distance from Pipe End (Top of Assembly), in
1	RTD 300"	RTD 809	230	packer borehole packer back end RTD	60.125	58.625
2	RTD 300"	RTD 809	230	packer borehole heater block 0 deg RTD	96.625	95.125
1	TC 300"	HSTC-TT-K-24S-300	250	temperature borehole plus 5	155.125	na
2	TC 300"	HSTC-TT-K-24S-300	250	temperature borehole plus 4	143.125	na
3	TC 300"	HSTC-TT-K-24S-300	250	temperature borehole plus 3	131.125	na
4	TC 300"	HSTC-TT-K-24S-300	250	temperature borehole plus 2	119.125	na
5	TC 300"	HSTC-TT-K-24S-300	250	temperature borehole plus 1	107.125	na
6	TC 300"	HSTC-TT-K-24S-300	250	temperature borehole 0 (aligned with center of heater block)	95.125	na
7	TC 300"	HSTC-TT-K-24S-300	250	temperature borehole minus 1	83.125	na
8	TC 300"	HSTC-TT-K-24S-300	250	temperature borehole minus 2	71.125	na
9	TC 300"	HSTC-TT-K-24S-300	250	temperature borehole minus 3	59.125	na
10	TC 300"	HSTC-TT-K-24S-300	250	packer borehole heater block end	99.75	98.25
11	TC 300"	HSTC-TT-K-24S-300	250	packer borehole heater block controller - packer borehole heater block 0 deg	96.625	95.125
12	TC 300"	HSTC-TT-K-24S-300	250	packer borehole heater block 90 deg	96.625	95.125
13	TC 300"	HSTC-TT-K-24S-300	250	packer borehole heater block 180 deg	96.625	95.125
14	TC 300"	HSTC-TT-K-24S-300	250	packer borehole heater block 270 deg	96.625	95.125
15	TC 300"	HSTC-TT-K-24S-300	250	packer borehole heater block plus 1	111.75	110.25
16	TC 300"	HSTC-TT-K-24S-300	250	packer borehole heater block plus 2	123.75	122.25
18	TC 240"	HSTC-TT-K-24S-240	250	temperature small borehole minus 2	70.5	na
17	TC 240"	HSTC-TT-K-24S-240	250	temperature small borehole minus 1	82.5	na
19	TC 240"	HSTC-TT-K-24S-240	250	temperature borehole minus 4	47.125	na
20	TC 240"	HSTC-TT-K-24S-240	250	temperature borehole minus 5	35.125	na
21	TC 240"	HSTC-TT-K-24S-240	250	temperature small borehole 0	94.5	22

22	TC 240"	HSTC-TT-K-24S-240	250	packer borehole mid-point heater packer	76	7
23	TC 240"	HSTC-TT-K-24S-240	250	packer borehole packer back end	60.125	8
24	TC 240"	HSTC-TT-K-24S-240	250	packer borehole packer front end	40.25	9
25	TC 240"	HSTC-TT-K-24S-240	250	packer borehole packer squeeze box	84.25	10
na	LVDT	Eddy Lab SM Series	200	LVDT for measuring packer borehole diameter	84.25	na

The thermocouples were connected to a Campbell Scientific, Inc. CR1000 and CR1000X dataloggers. A Campbell Scientific, Inc. thermocouple multiplexer model AM25T was used as part of the temperature measurement process.

3.6. Design of Phase 1 Borehole Deformation Gage

Borehole closure gauges are used to accurately measure changes in the radial dimension of a borehole in multiple directions to identify the closure of the borehole. In order to obtain these measurements, a borehole deformation gauge was developed for this set of experiments. The gauge was designed based on a survey of downhole equipment used in the oil and gas industry and past experience with similar measurements that were made at both WIPP and Yucca Mountain. Of prime concern was the ability of the tool to withstand being moved within the borehole without getting hung up on the wall of the borehole or mineral deposits which have precipitated from brine inflow into the borehole. The tool is initially positioned in the borehole by being pushed in with the heater and packer assembly and may be subsequently repositioned when the assembly is repositioned or re-installed. The gauge was also built within the financial and time constraints of the project at the time. The final design concern was confirming that the measurements were centralized to ensure the average borehole deformation is evaluated. An off-center diameter measurement could be prone to a higher amount of error, so it was preferred to make one with four contacts points around the circumference of the borehole.

With these considerations in mind, the design of the borehole deformation gauge was based on borehole centralizers and borehole deformation gauges used in the petroleum industry. A picture of the device is shown in **Figure *6***. A schematic drawing with dimensions is provided in Appendix 1. The gauge is built around a 1-inch Schedule 40 stainless steel pipe. Four bow springs are used to centralize the gauge in the borehole and deflect as closure of the borehole occurs. The bow springs are made of blue tempered AISI 1095 spring steel. The defection of the bow springs causes the sliding end collar, made of PEEK plastic, to slide along the stainless steel pipe component. The amount of sliding is measured by a linear variable differential transformer (LVDT). An LVDT from eddylab GmbH with a measurement range of 5 mm was used. The LVDT was chosen based on its ease of use, size, and ruggedness. The LVDT has an operating temperature range up to 120 °C (optional 200 °C) and IP68 rating of 10 bar (145 psi). Calculations based on a simplification of the bow springs' deflection due to borehole closure suggested that the movement of the sliding end of the gauge will be linear over a range much larger range than that anticipated in the field test. Calibration was performed using a 0.010 inch (0.254 mm) thick × 3 inches (76.2 mm) wide × 18 inches (457 mm) long coiled strip of stainless steel shim material which was marked at various lengths corresponding to known diameters. The movement of the sliding end collar was indeed determined to be linear throughout the range of different diameters used during the calibration of the borehole deformation gauge.

The sliding end collar is made from a PEEK (polyether ether ketone) plastic bushing. PEEK is semicrystalline thermoplastic with excellent mechanical, wear, and chemical resistance properties that are retained to high continuous temperatures (260 °C, 500 °F). Movement of the sliding end collar is further enhanced by the application of Krytox grease between the stainless steel pipe and PEEK bushing. A stainless steel key in the pipe component and groove in the PEEK bushing is used to help maintain a straight back-and-forth movement, and keep the bow springs from twisting and possibly bending out of shape.

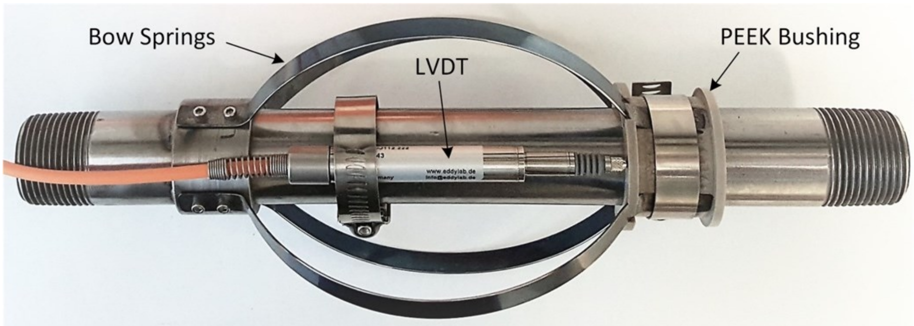

Figure 6. Picture of the Phase 1 LVDT device constructed to measure borehole closure

Calibration was performed using a 0.010 inch (0.254 mm) thick × 3 inches (76.2 mm) wide × 18 inches (457 mm) long coiled strip of stainless steel shim material which was marked at various lengths corresponding to known diameters. The measurement of the movement of the sliding end collar is made using a linear variable differential transformer (LVDT) from eddylab GmbH with a measurement range of 5 mm.

3.7. Design of Phase 1 Packer Assembly and Instrumentation

The packer system was designed to isolate the heated borehole from the access drift. The packer included several pass-through tubes designed to access the isolated interval of the borehole, including reading of the pressure behind the packer for gas permeability measurements. The detailed design and construction of the packer is provided in Appendix 1. A drift view of the packer system during initial testing, before installation of the heater, thermocouples, and other components, being placed into borehole SNLCH112 is shown in ***Figure 7***.

Figure 7. Pre-assembly test of Phase 1 packer system used to isolate the heated borehole from the access drift.

3.8. Design of Phase 1 Moisture Collection and Permeability Measurement System

Figure *8* shows the moisture collection system and gas permeability measurement system in a simplified schematic.

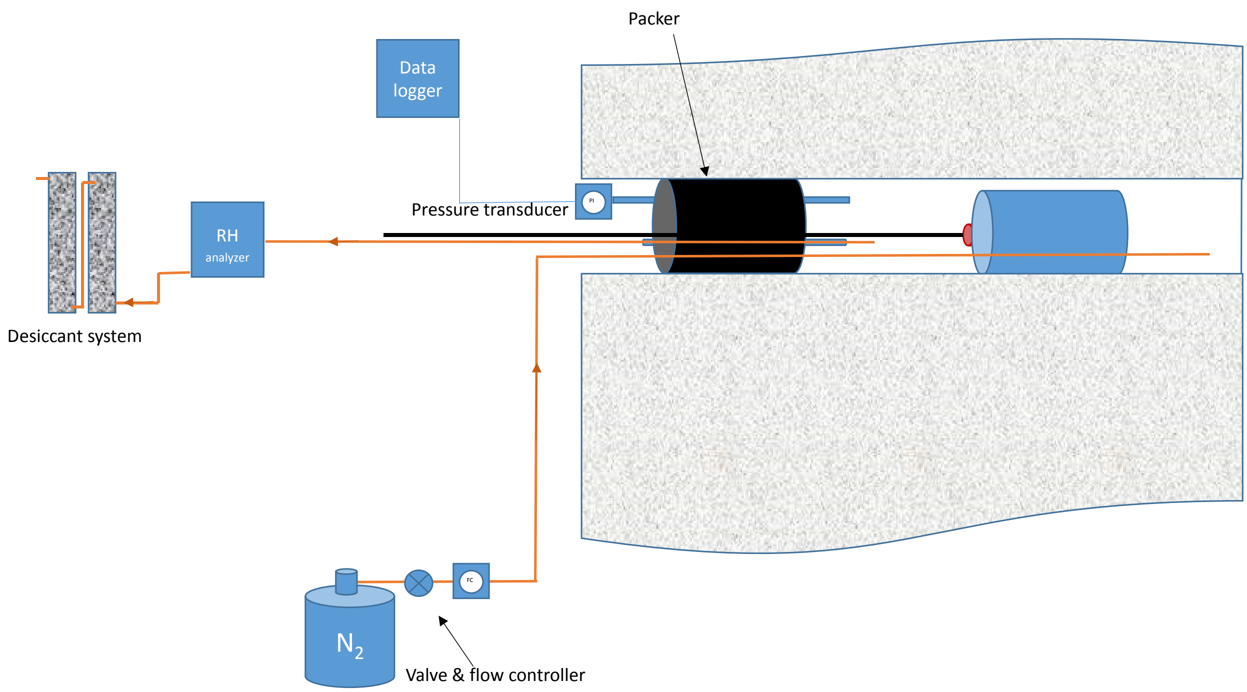

Figure 8. Simplified diagram showing the Phase 1 moisture collection and gas permeability measurement systems.

The system circulates dry nitrogen behind the heater block to drive moisture toward a relative humidity (RH) analyzer and desiccant system downstream. The nitrogen flow rate is controlled by a flow controller placed on the inlet tube. The technical details of the components of the moisture collection system are described in more details in Appendix A. The packer, nitrogen bottle, and plumbing are also used to characterize the gas permeability of the borehole/packer system. To perform permeability measurements, the ports connecting the packer to the moisture collection system are sealed and the pressure of the packer set to 50 psi while the pressure of the gas behind the packer is set to 30 psi. After the pressure is stabilized to 30 psi the nitrogen valve is shut to restrict flow and the pressure decay is recorded by a pressure transducer that is connected to the isolated interval behind the packer by a pass-through valve. The permeability of the formation is calculated by fitting the pressure decay curve using a 3D model that assumes a fixed permeability value.

3.9. Design of Phase 1 Brine Collection System

A pass-through to allow insertion of a tubing for brine collection was built into the packer system. The collection system consists of a Teflon tube (1/4" diameter) that is connected to a 3/8" diameter pass-through. The Teflon tube extends to the end of the borehole. A small diameter, rigid Teflon tube (1/8") is inserted into the 1/4" Teflon tube to sample brine that might accumulate at the back of the borehole. When not in use the smaller diameter Teflon tube is removed and the port is sealed with a Swagelok fitting.

A 3D rendering and a real picture of train assembly constructed with all components is shown in ***Figure 9*** and ***Figure 10***.

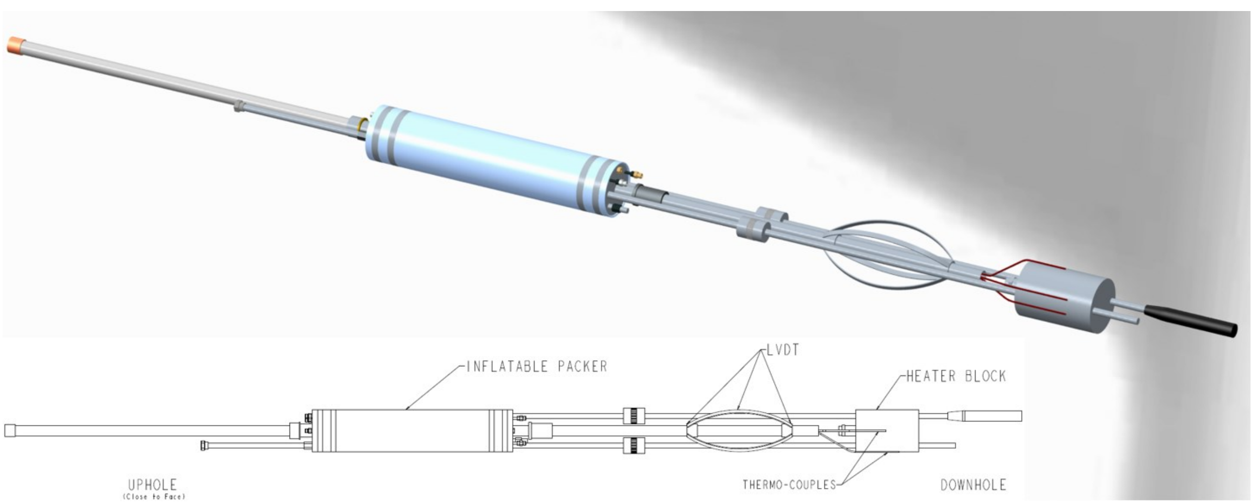

Figure 9. As-built rendering of Phase 1 heater/packer assembly.

Figure 10. The Phase 1 heater/packer assembly prior to installation.

3.10. Design of Phase 1 ERT System

A schematic representation of the ERT system is shown in **Figure *11***. A small-diameter resistive cartridge heater element (McMaster-Carr 1000-watt Cartridge Heater with Internal Temperature Sensor), controlled by a Stanford Research Systems (SRS, Model PTC10) temperature controller, will be installed in a central borehole and backfilled/grouted. Up to 16 stainless steel electrodes will be emplaced a few inches apart along each of the two electrode boreholes, mounted on the outside of small-diameter PVC tubes, and grouted in place (WIPP grout recipe contains cement, attapulgite, salt, and water). These electrodes will be connected to the ERT controller, which will use them as both current sources and electrodes for voltage measurements, during different parts of each ERT survey. We expect to conduct the experiment for a week depending on the trajectory of the system evolution during heating. Unattended continuous monitoring will occur during off-hours in order to evaluate electrical potential evolution.

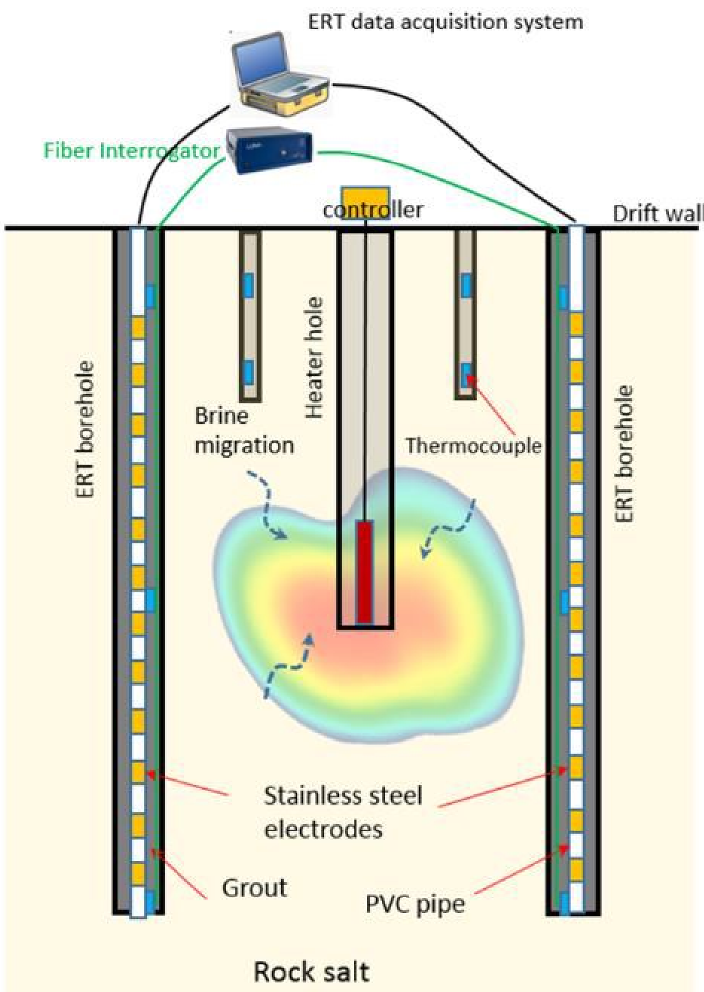

Figure 11. Schematic cross-section of the Phase 1 ERT data acquisition layout.

The annulus of the electrode boreholes (between the PVC pipe and borehole wall) will be filled with grout. The grout must cure prior to beginning the test to ensure the electrodes have a good electrical connection with the salt. The MPT DAS-1 Electrical Impedance Tomography System is the ERT controller and will provide the current source and data acquisition. The heater temperature will not exceed 120°C.

3.11. Phase 1 Data Logging

The thermocouples, RTDs, and LVDT borehole closure system were connected to Campbell Scientific, Inc. CR1000 and CR1000X dataloggers. A Campbell Scientific, Inc. thermocouple multiplexer model AM25T was also used for temperature recording.

4. Phase 1 Testing Summary

Phase 1 testing was intended to build confidence and to test instrumentation including gas permeability measurements, the heater assembly effectiveness, and the moisture collection and brine sampling systems.

4.1. Phase 1 Gas Permeability Measurements.

Gas permeability measurements are used to measure changes in borehole permeability to identify the evolution or creation of air-filled porosity or fractures within the rock salt. The permeability tests can only be performed if all ports on the face of the packer are properly sealed. Sealing was checked with a soap solution and connections were tightened until bubbles were not produced. Gas permeability measurements were performed to assess the permeability of the existing borehole SNLCH112 at three times: 1) before heating, 2) during heating, and 3) after heating. To perform the permeability test, the region behind the packer in borehole SNLCH112 was pressurized to a total pressure of 45 psi (3 atm of total pressure, or two atm of overpressure). During all permeability tests, the packer was inflated to 50 psi to isolate the borehole behind the packer (in the region containing the heater) from the WIPP access drift and allow pressure to build up in the test section of the borehole. During the testing, the packer was located between 1.0 and 1.5 meters from the drift wall (see schematic representation in ***Figure 12***).

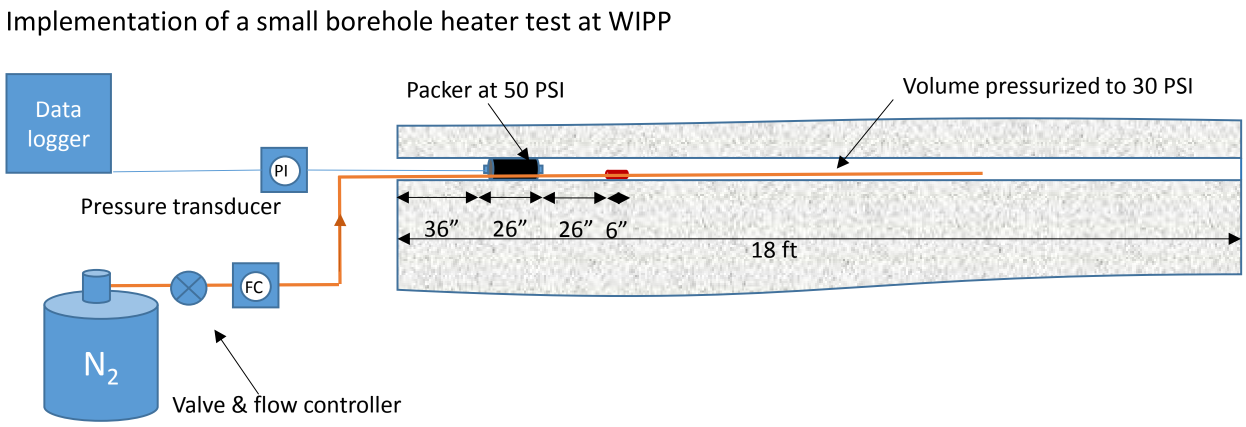

Figure 12. Schematic diagram showing the Phase 1 setup used for gas permeability measurements.

After the borehole was pressurized, the valve on the nitrogen tank was closed so that pressure decay could only be caused by gas seepage through the salt wall and/or packer. The pressure decay on the downhole (heater) side of the packer is measured through a pressure transducer connected to a datalogger that continually records the pressure in the isolated interval of the borehole. The pressure decay data for the three permeability measurements are shown in **Figure *13***. The measurements on 7/19/2018 are before heating, 8/13/2018 are during heating, and 8/21/2018 are after heating. All three sets of measurements show similar behavior with pressure decay happening over the span of 0.2 days.

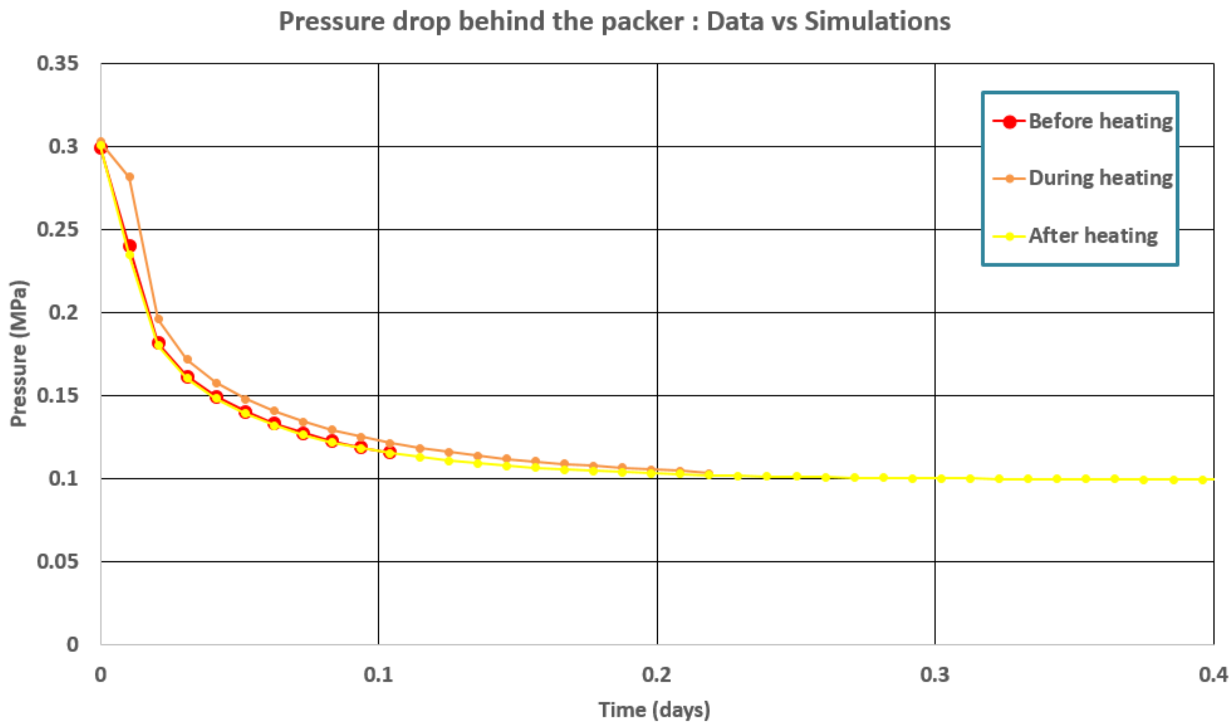

Figure 13. Experimental data results showing the pressure decay recorded during Phase 1 permeability testing.

4.2. Phase 1 Moisture Collection and Brine Inflow Measurements

Brine is available in the salt formation in the form of brine inclusions, as intergranular brine, and as water associated with hydrous minerals in the salt. Thermal gradients, dilation, and fracturing of the salt formation are known to facilitate brine migration. The chemical composition of the brine is also affected by brine transport. One of the main objectives of the heated borehole test is to quantify brine inflow into the isolated borehole interval as a function of the temperature, pressure gradient, and heat gradient developed in the rock salt. It is also of great interest to develop an understanding of how the chemical composition of the brine in the borehole is affected by contributions from the three water sources in salt. The experimental setup designed to quantify brine inflow and to collect brine samples is described in Section 3.8 and in Appendix A. The initial testing described here was designed to test the viability of the experimental setup. The experiments were setup to examine brine inflow under isothermal conditions at ambient temperature flowed by examinations of brine inflow under constant heating at a set point of 120^{o}C. Quantification of brine inflow under isothermal conditions were setup by eliminating all available brine that ponded at the back of the borehole using a vacuum cleaner with a long hose and the isolation of the borehole from the drift area. We used dry nitrogen (99.999% N_2) as a carrier gas to sweep the isolated interval of the borehole and drive any available moisture toward a small polycarbonate chamber equipped with a relative humidity probe that monitors the RH continually. The nitrogen gas existing the RH analysis chamber is redirected towards two cartridges filled with a desiccant that scavenges moisture carried by the carrier gas. The weight of the cartridges was measured daily or as often as access to the underground experiential area at WIPP permitted. Total moisture released from the isolated interval of the borehole was determined by integrating the flow rate and RH readings over the duration of the experiment. The moisture accumulated in the desiccant cartridges is compared to the RH data for validation.

The data in **Figure *14*** show plots of the RH (green line) over a period of active monitoring. The flow rate was maintained at 200 mL per minute for most of the monitoring duration and completely stopped after 8/17/18. The temperature of the heater in the isolated borehole interval is shown in (blue line) for the same monitoring period. The total extracted moisture captured by the desiccant cartridges is represented by the orange line.

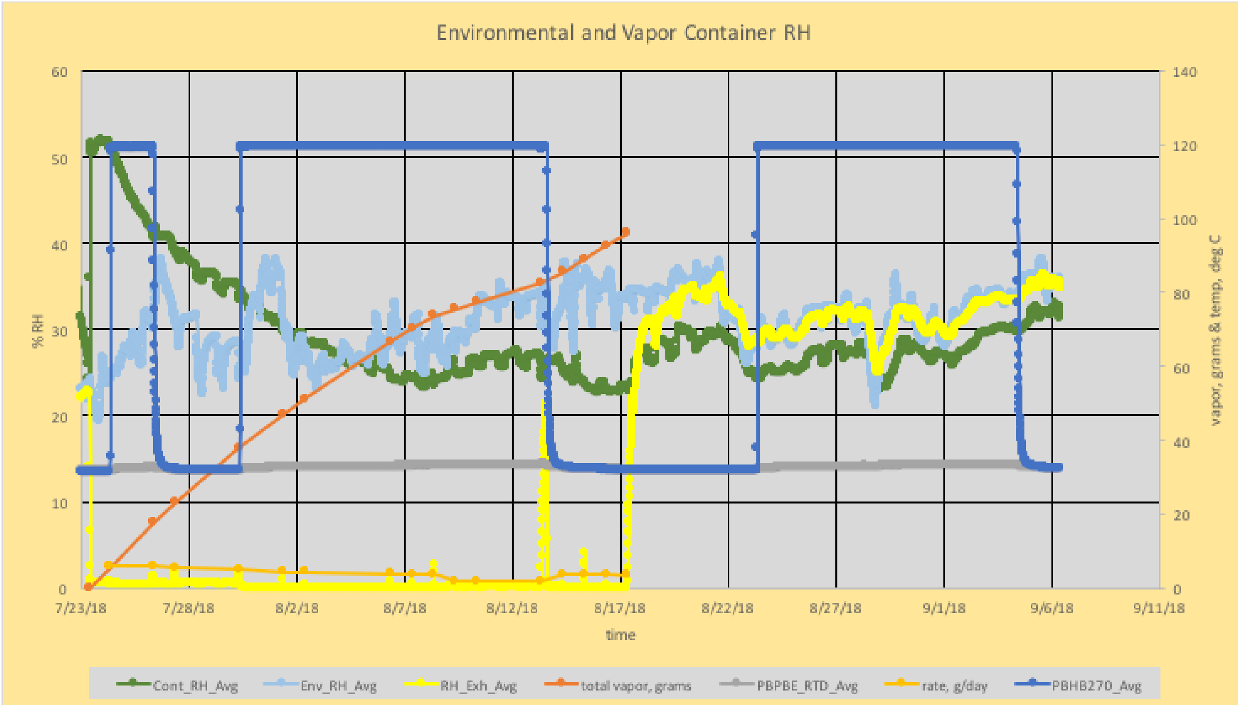

Figure 14. Plot showing water extraction by nitrogen circulation through the isolated interval of the borehole (Phase 1).

The RH plot shows that the reading of the RH of the nitrogen gas exiting the isolated borehole interval decreases from about 50% to about 28%. The initial elevated RH is due to the brine saturating the porosity of the salt in the borehole wall that was present before the start of the borehole isolation. After the initial period of high RH (~50%), the moisture content in the nitrogen stabilized and fluctuated between 20 to 30% RH. There is no obvious correlation between the heater temperature and the RH of the nitrogen gas sweeping the isolated interval of the borehole. The rate of moisture accumulation in the desiccant cartridges was almost constant throughout the entire testing period (**Figure *15***) and averaged 4.2 g/day.

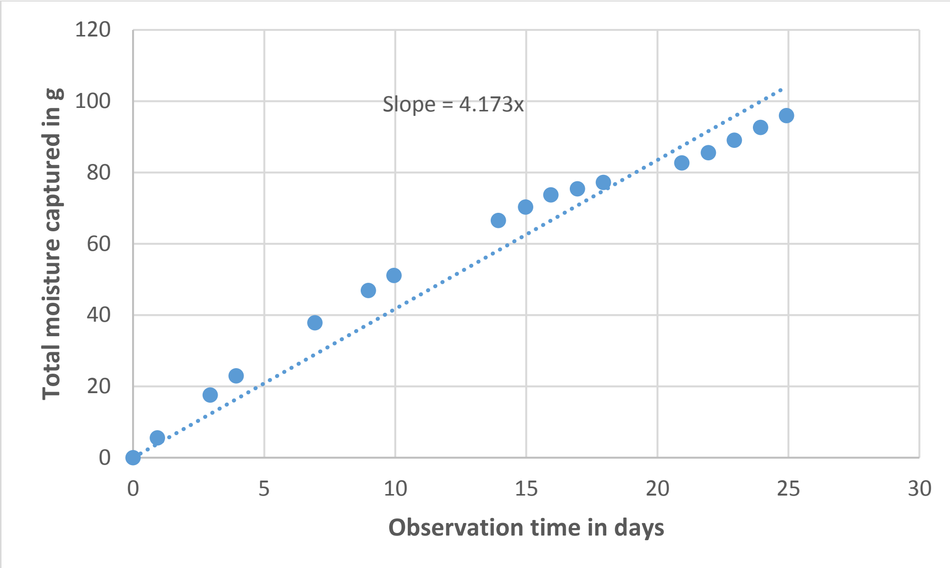

Figure 15. Plot of the total moisture captured by the desiccant cartridges as a function of observation days (Phase 1).

If we assume an average RH of 30 % for the entire observation time and a temperature of 100°F which is close to the measurements shown in **Figure *14***, then the total moisture carried by the dry nitrogen is estimated to 103 g over the entire observation period. This estimation was calculated by assuming an air density of 1.2 kg/m^3 , a flow of 200 mL/min (7.7 m^3) over the observation time, and a water content of 0.012 g/L. The daily average moisture capture is estimated to be 4.14 g/day. This average is almost identical to the number determined from the weight of the desiccant cartridges shown in **Figure *15***. The moisture capture using the desiccant cartridges and the RH measurement probe are consistent. However, the lack of an enhanced brine inflow into the borehole during periods of heating is not consistent with our initial assumption. This is due to the lack of coupling between the heater and salt formation which resulted in an inefficient heating of the salt (i.e., only a small temperature rise). The data presented in the next section, which document the evolution of the rock salt temperature as a function of the heater temperature, supports this interpretation.

We were unable to collect any liquid brine from the back of the borehole during the testing period. This is due to the low volume of brine inflow into the borehole and constant sweeping of the isolated borehole interval with nitrogen which prevented brine accumulation.

4.3. Phase 1 Heater Controlled to a Set Point Temperature

The technical details of the heater block assembly and positions of the thermocouples and RTDs deployed in and around the borehole to monitor temperature during heating are presented in section 4.1.3 and Appendix A. A schematic representation of the heater and temperature probes is shown in ***Figure 16***.

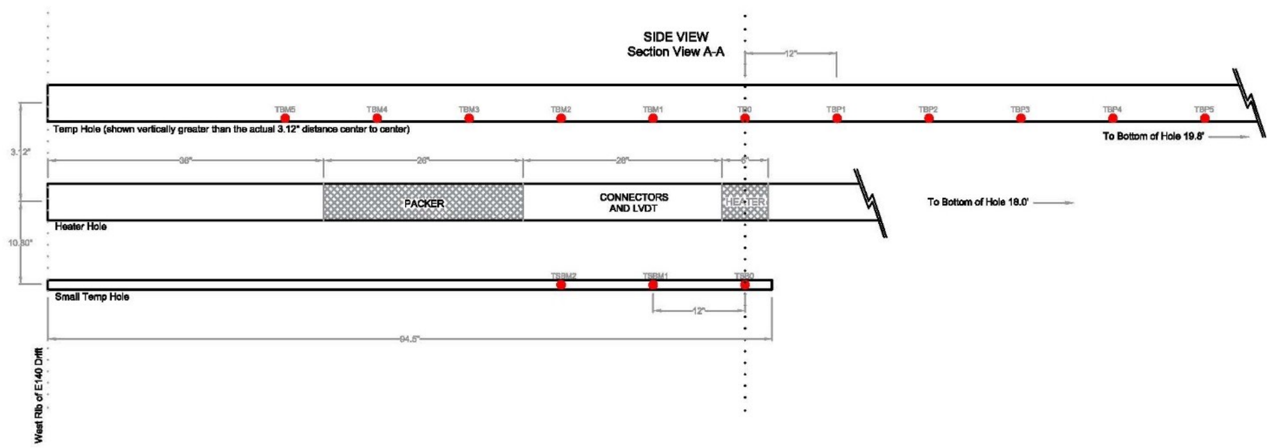

Figure 16. Schematic representation of the positions of the Phase 1 temperature probes.

A schematic representation of the positions of the temperature borehole and temperature small borehole relative to the packer borehole is shown in ***Figure 17***.

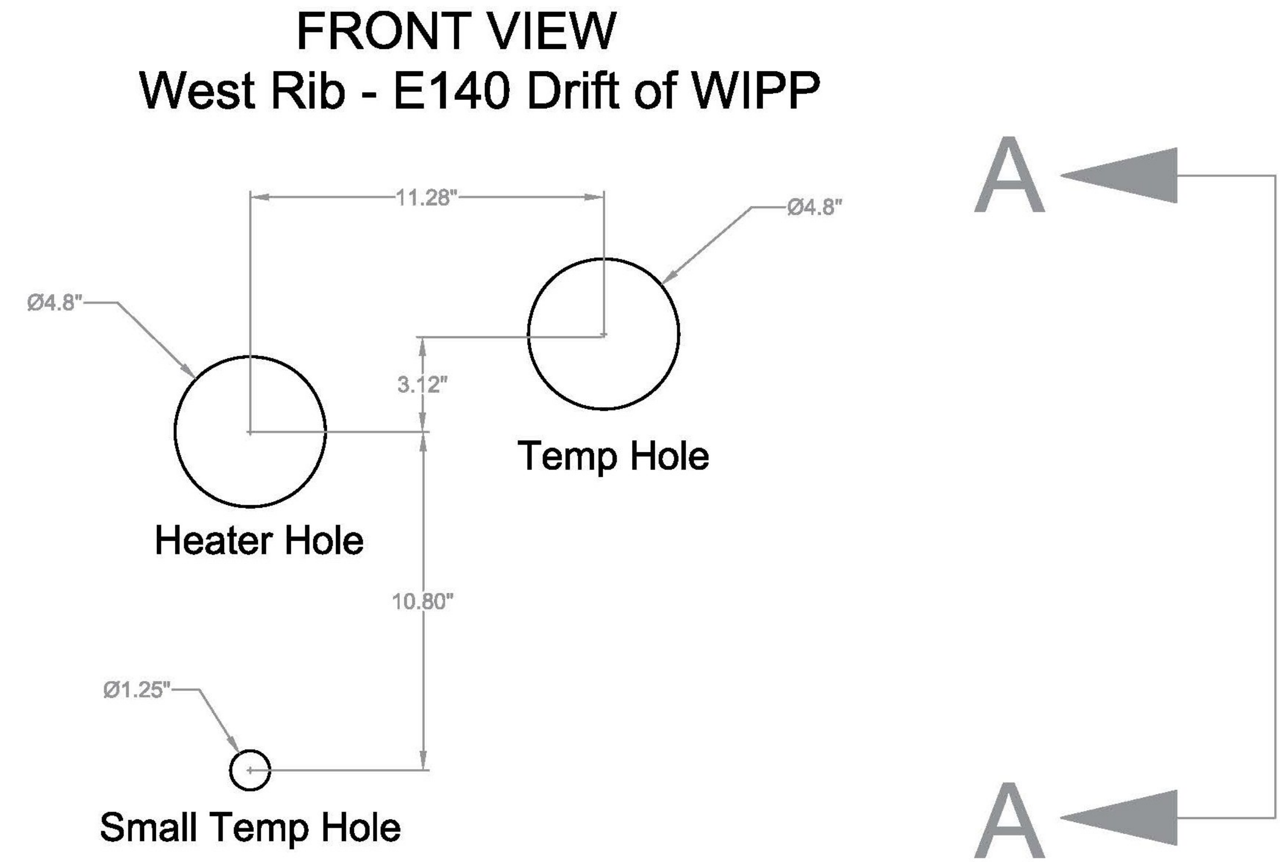

Figure 17. Schematic representation of the layout of the different boreholes instrumented in Phase 1 testing.

The heater block temperature is controlled by a temperature controller that controls the applied heater power to maintain a fixed temperature at a chosen thermocouple. Several heating tests were performed by setting the heater block to 120 ºC to test the viability of the experimental setup designed and to provide initial experimental data for model verification. The plots in **Figure *18*** show the temperature profiles during several heating events recorded by thermocouples and RTDs positioned at different distances from the heater in the heated packer borehole. The data show a very rapid response of the heating assembly (PBHB0). Equilibrium is reached in less than an hour. However, the temperatures drop off significantly a short distance away from the heater block in all directions. The temperature in the isolated interval past the heater (PBHBP1 and PBHBP2), which are positioned at 1 ft and 2 ft from the center of the heater block never exceed 36.5ºC (less than 4 degrees C above ambient). It is also the same for the temperatures before the heater (PBPM, PBPB, PBPF). These temperatures are the same as the drift temperatures and indicate the heater setup lacks effectiveness to heat the air temperature in the isolated interval of the borehole.

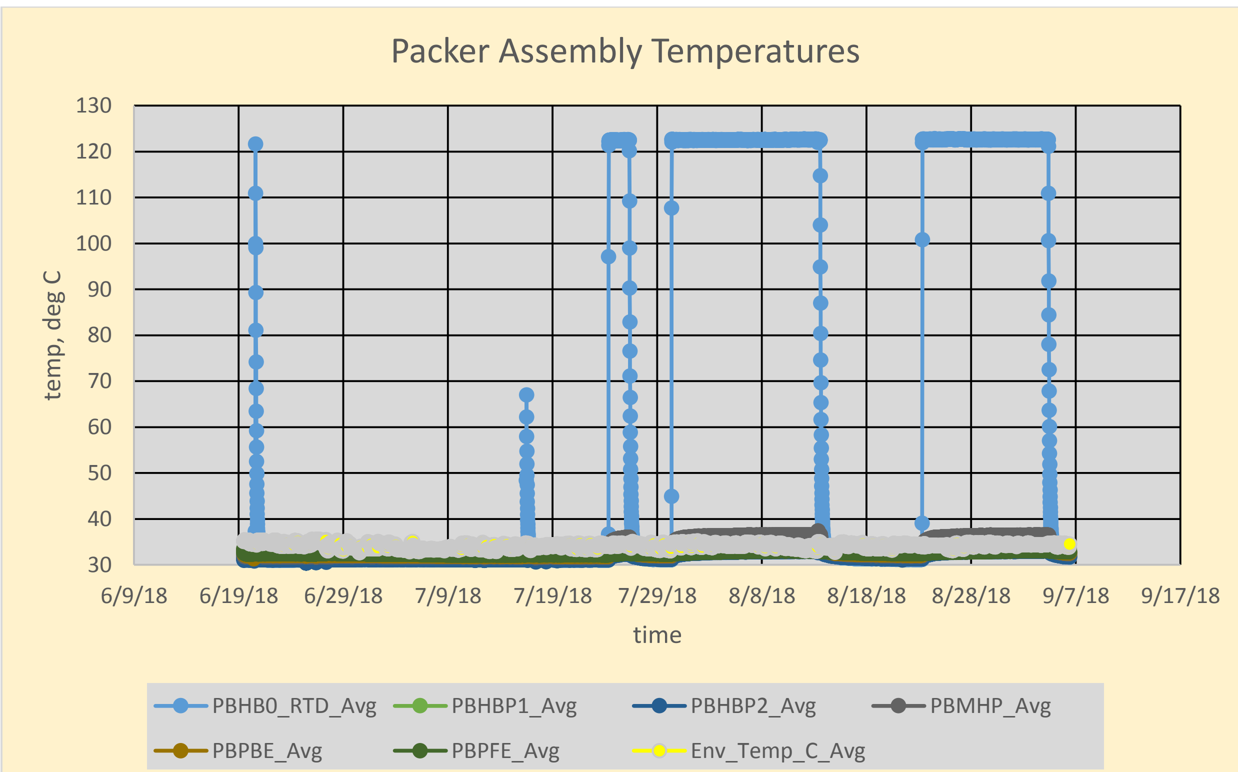

Figure 18. Phase 1 temperature profiles recorded by thermocouples and RTDs during the heater test in the heated packer borehole. The different colored lines represent individual thermocouples and RTDs positioned at different distances from the heater.

The plot in **Figure *19*** shows the evolution of the temperatures in two monitoring boreholes situated at 11.3 inches horizontally to the right (TB) and 10.8 inches below the heater borehole (TSB) (**Figure *17***). The data show a large delay between the response of the heater block and the temperatures at the wall of the observation borehole. The temperature does not reach steady state even after more than ten days of continuous heating. The amplitude of the temperature increase is also significantly smaller than expected. The temperature at TB0, which is immediately below the heater, increased by less than 4 degrees in 10 days of continuous heating. Thermocouples positioned at 1 ft past the heater indicate less than one degree of temperature increase. All thermocouples are reading temperatures below the ambient drift temperature which is anomolously high because of the low flow of air in the drift area.

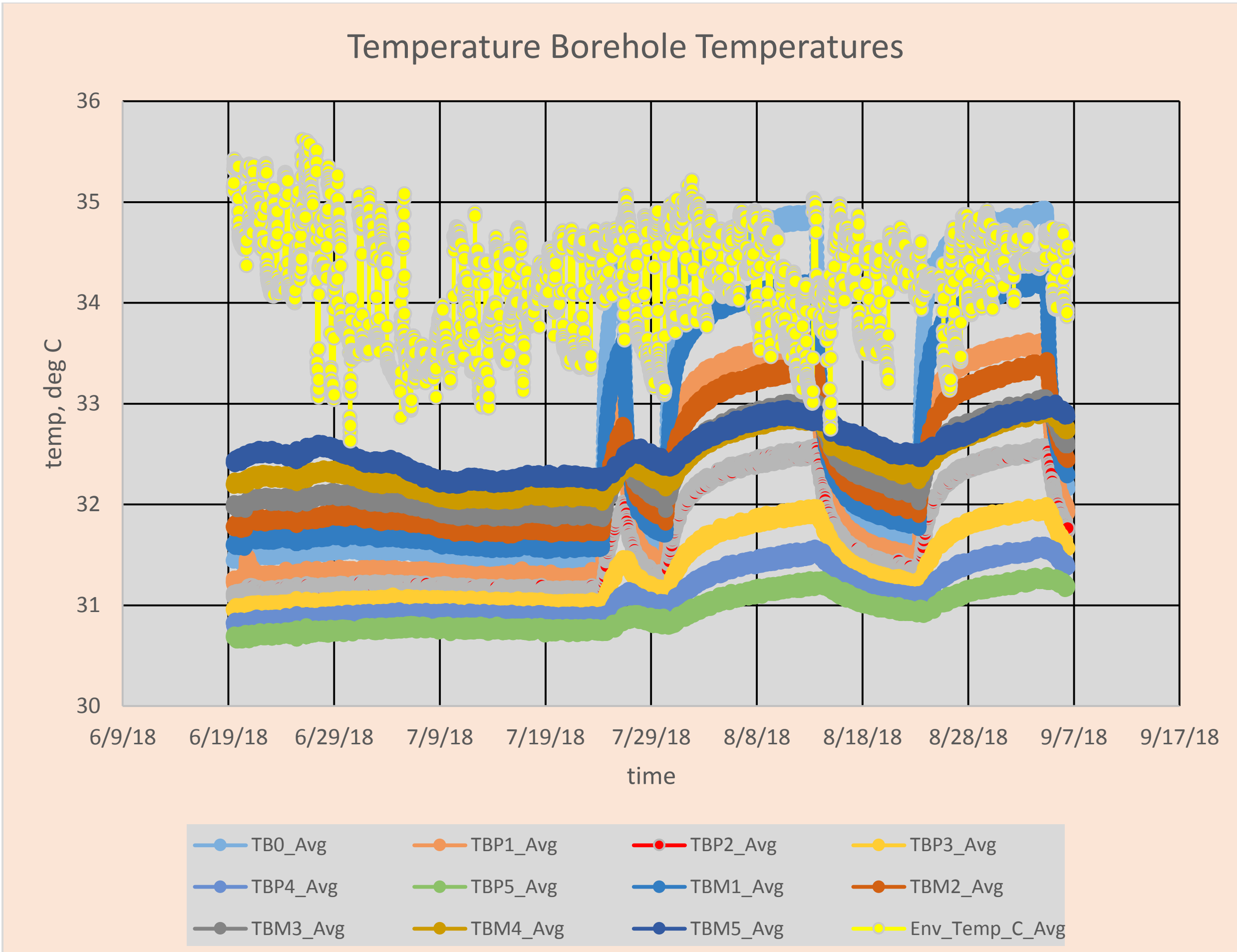

Figure 19. Temperature profiles recorded by thermocouples and RTDs during the heater test in the temperature borehole. The different colored lines represent individual thermocouples and RTDs positioned at different distances from the heater.

Temperatures in the small observation borehole (TSB) situated at about 10 inches immediately below the heater (See **Figure** *17*) are shown in ***Figure 20***. The temperatures are consistent with the temperatures recorded in the temperature observation borehole shown in ***Figure 19***. The thermocouple in contact with the wall directly below the heater recoded the greatest temperature increase, however the increase is less than 4 degrees. All the remaining thermocouples recorded minor temperature increases. The temperature in the rock salt did not increase significantly and is well below model predictions made before the test was implemented.

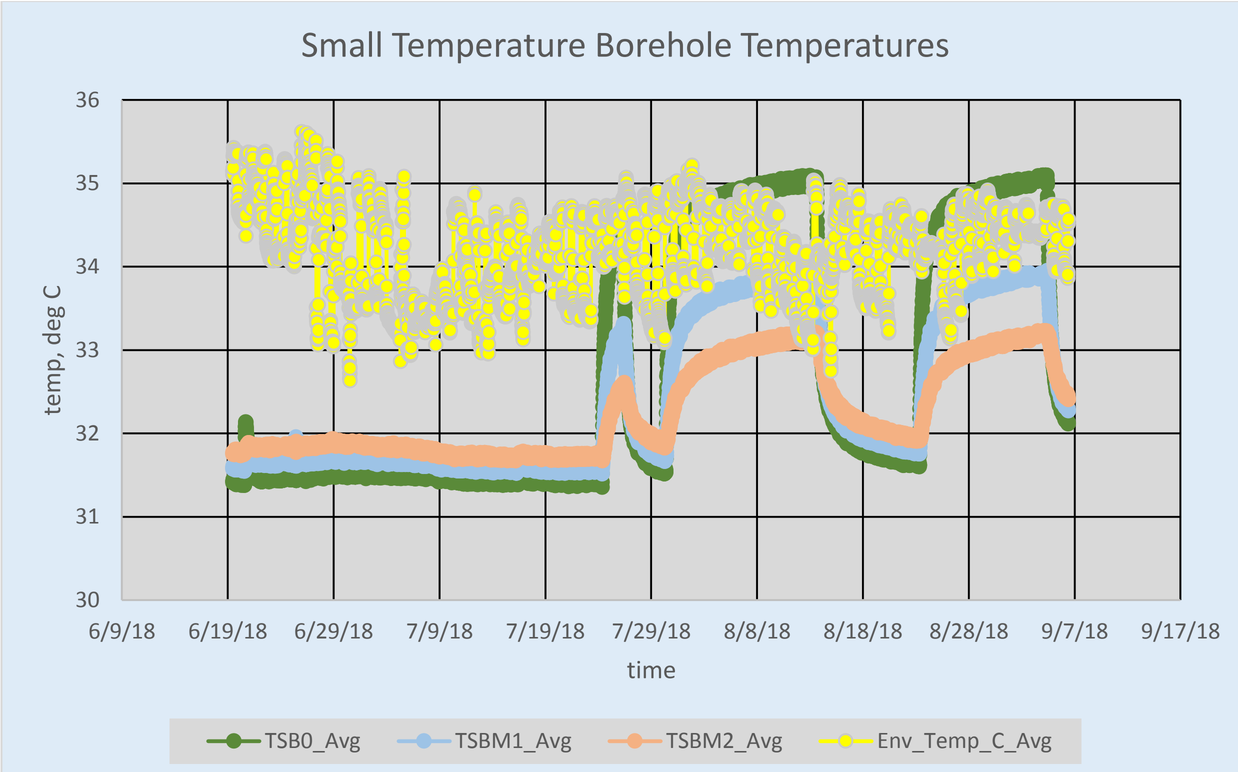

Figure 20 Temperature profiles recorded by thermocouples and RTDs during the heater test in the small temperature borehole. The locations of the temperature probes are shown in Figure 16.

5. Simulations of the Phase 1 Thermal Test

5.1. Simulation details

We compare results from the borehole heater shakedown testing with output from numerical simulations performed using FEHM. A complete description of the equations in FEHM, including specific modifications for salt can be found in Johnson et al, [**17**] and references therein.

The numerical mesh used for all simulations is three dimensional and centered on Borehole SNLCH112 at x = 0 z = 0 (**Figure 21**). In the directions of the drift face, the mesh extends 1.52 m away from the center in each direction, with up and right being positive values of z and x respectively. The mesh extends from the face of the drift wall 7 m into the rock salt as shown in

Figure 22. The mesh has 238107 volume elements with volumes ranging from 7.05×10^{-4} m^3 in the far-field to 1.86×10^{-6} m^3 in the center of the borehole.

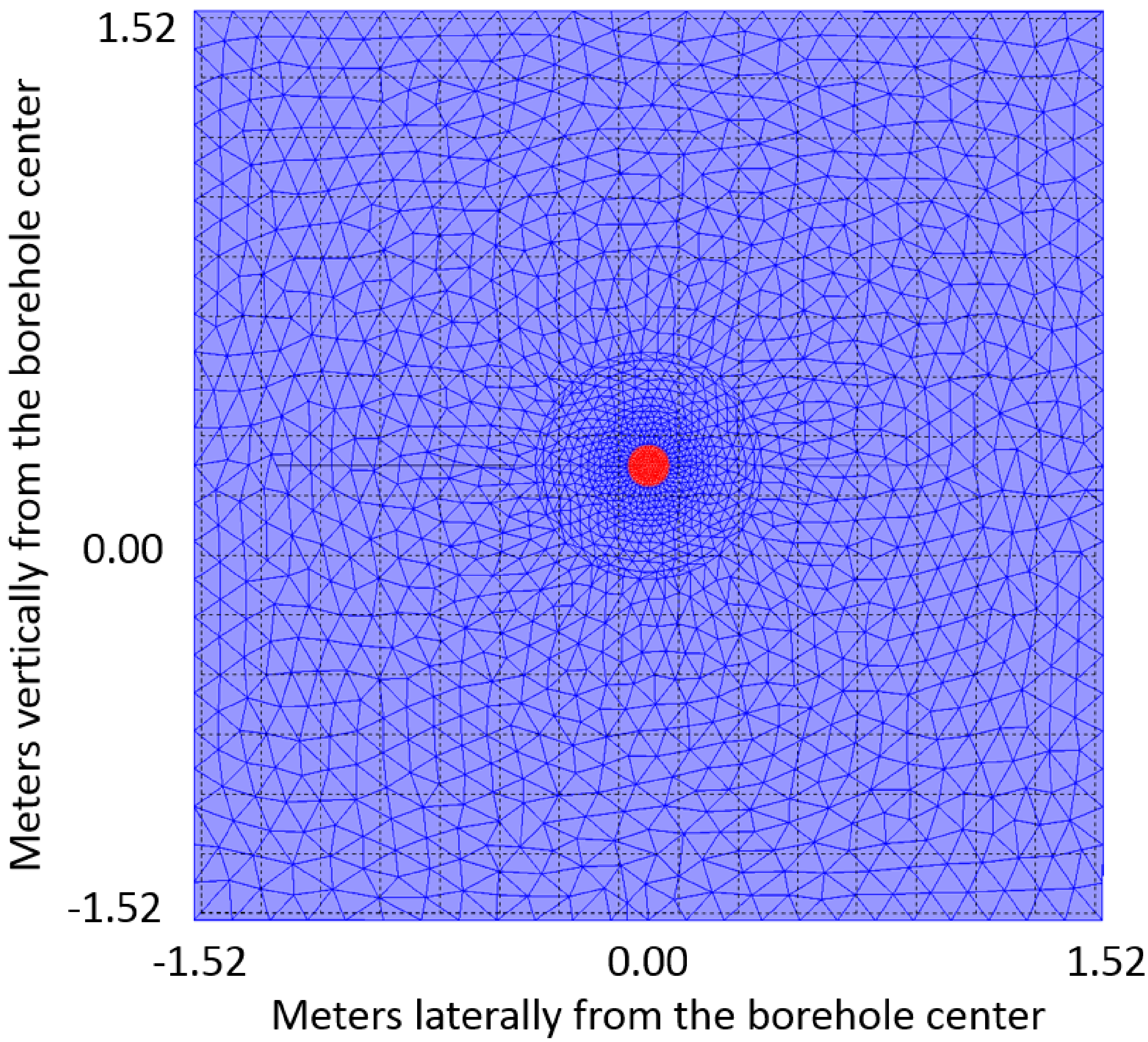

Figure 21. Drift face view of the numerical mesh showing the borehole as red with the rock salt as dark blue.

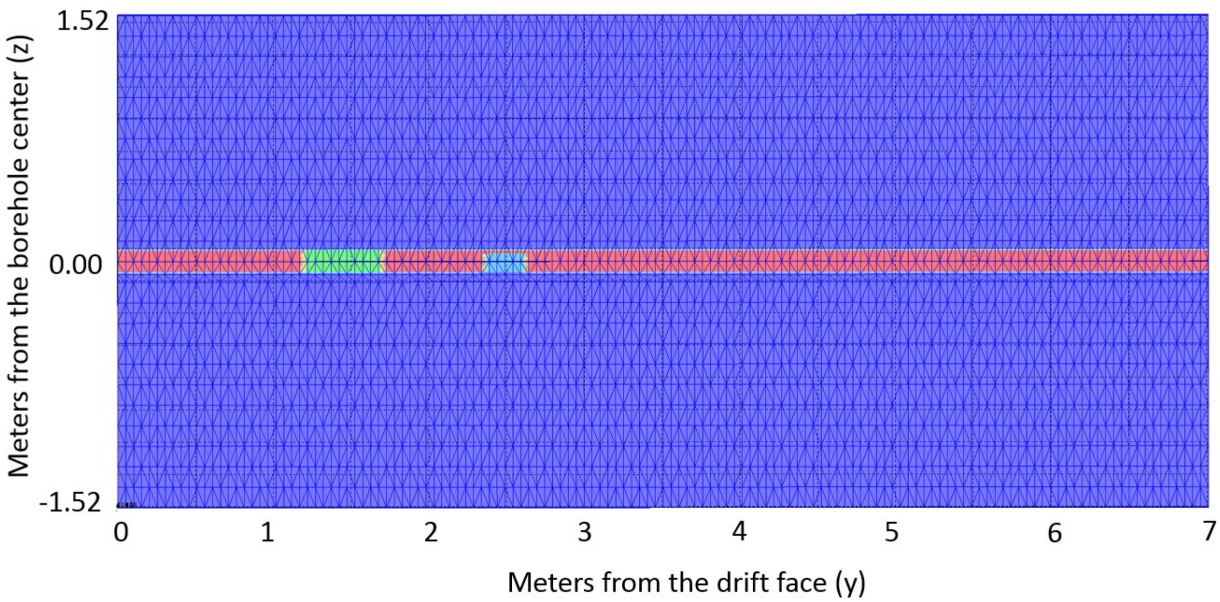

Figure 22. Side view of the numerical mesh showing the borehole as red with the packer interval as green and the heater as light blue. Rock salt is dark blue.

Initial material properties are given in ***Table 3***. The variable thermal conductivity of the rock salt follows the function described in [**17**] and references therein.

Table 3. Material properties of the simulations

	Porosity	Density (kg/m^3)	Thermal conductivity (W/(m K))	Heat capacity (J/(kg K))	Permeability (m^2)
Rock Salt	0.001	2170	Variable	931	1×10^{-20}
Air	-----	1	0.06	1000	1×10^{-12}
Packer	0.9	300	1	500	1×10^{-26}
Heater	0.001	8000	15	1000	1×10^{-12}

5.2. Simulations of Phase 1 Pressure Decay.

For pressure decay, the simulations are run in isothermal mode at 31.5°C, the nominal average background temperature. Pressure in the model is initially 0.1 MPa (1 atm) and the pressure is increased in the borehole interval behind the packer (y=1.5-7m) to 0.3 MPa (3 atm). Simulations were performed to determine what permeability in the simulated rock salt could match the measured pressure decay data. Even with an unrealistically high permeability in the simulated rock salt (1 x 10^{-14} m^2), the shape and decay rate of the pressure behind the packer were not close to measured data (**Figure 23**). We next specified a more typical value for rock salt permeability (1 x 10^{-20} m^2) and ran a simulation to see if leakage through the packer could explain the data. For this simulation, the packer was given a low porosity (0.001) and a high permeability (1 x 10^{-11} m^2). Results from this simulation match the data well and imply that we were not able to fully seal the packer pass through ports (**Figure 23**, curve labeled SIM 1e-11 m2 Packer perm). The small leak is most likely due to the number of wires passing through the central 1" pipe and the epoxy seal that was used in this pass-through.

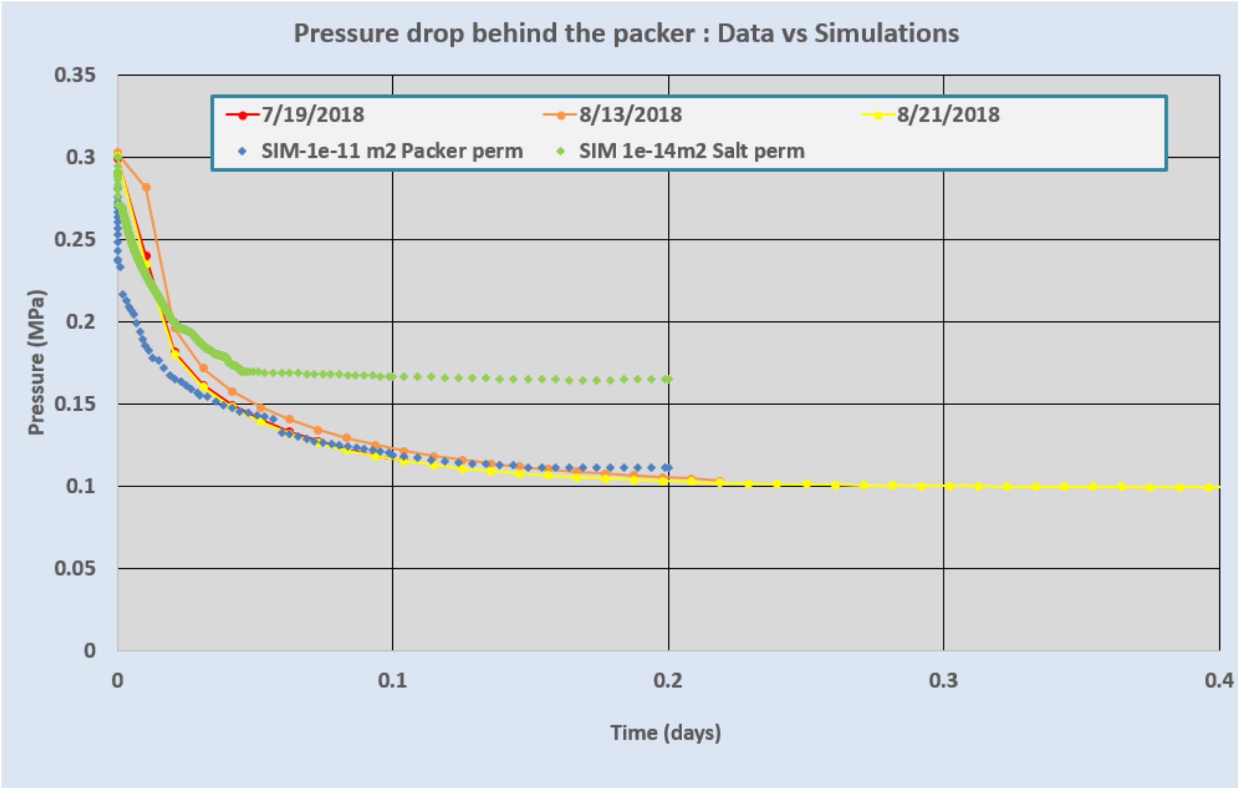

Figure 23. Phase 1 experimental pressure decay compared to simulation results.

5.3. Simulations of Phase 1 Moisture Removal

In the moisture removal simulations, two nodes are added to represent the nitrogen inlet and gas outlet as implemented in the experiment. The inlet node (101068) is located behind the packer, in the center of the heater borehole, 3 m from the drift face (y = 3.0 m). The gas outlet node (66812) is located just past the downhole face of the simulated packer at y = 1.98 m. A fixed gas flow rate of 200 mL/min (3.33 x 10-6 kg/s) is applied to the inlet node. The inlet node water vapor concentration is fixed to zero. The outlet node is specified to maintain the original pressure of 0.1 MPa (1 atm) and any gas leaving the domain will carry with it the water vapor and thermal energy associated with the temperature and relative humidity of the outlet node. ***Table 3*** includes the properties used in the moisture removal simulation, however in the simulation the rock salt permeability is 1 x 10^{-22} m^2. The initial saturation for the rock salt for this simulation is 0.9. The simulation results are from a single forward run using initial guesses for material properties, with constant heating of 120°C.

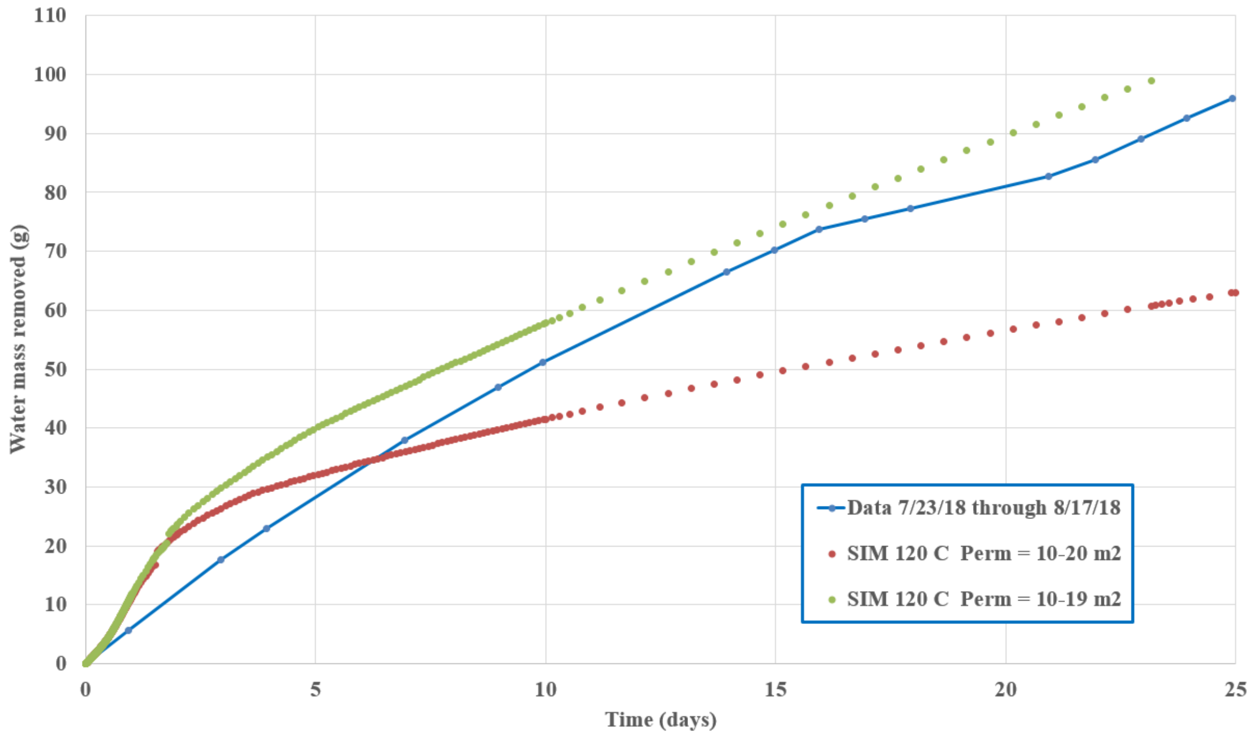

Figure 24. Water mass removal through the nitrogen flow system, Phase 1 data vs simulations.

The initial rate of water removal during the first few days in the simulation compares well to the data, however the late time behavior of the simulation yields a lower rate of water removal than seen in the data (***Figure 24***). Permeability of the rock salt was then modified to 1 x 10^{-19} m^2 and the simulation was rerun. Results from this simulation, shown in green on **Error! Reference ource not found.**, track the measured mass removal at later times, 10-25 days, quite well.

A major differences between the initial simulation and the experiment include periods when the heater was turned off during the experiment, however we are still working to obtain convergence on these more complicated simulations. Additionally, the rock salt walls of the borehole likely have higher permeability due to damage induced by drilling. Increased permeability in the rock salt surrounding the borehole could allow water to migrate toward the borehole where it would be available for evaporation by the dry nitrogen. We plan to explore a series of additional simulations to determine what parameters may lead to better long term match to the experimental data.

5.4. Simulations of Phase 1 Temperature Changes

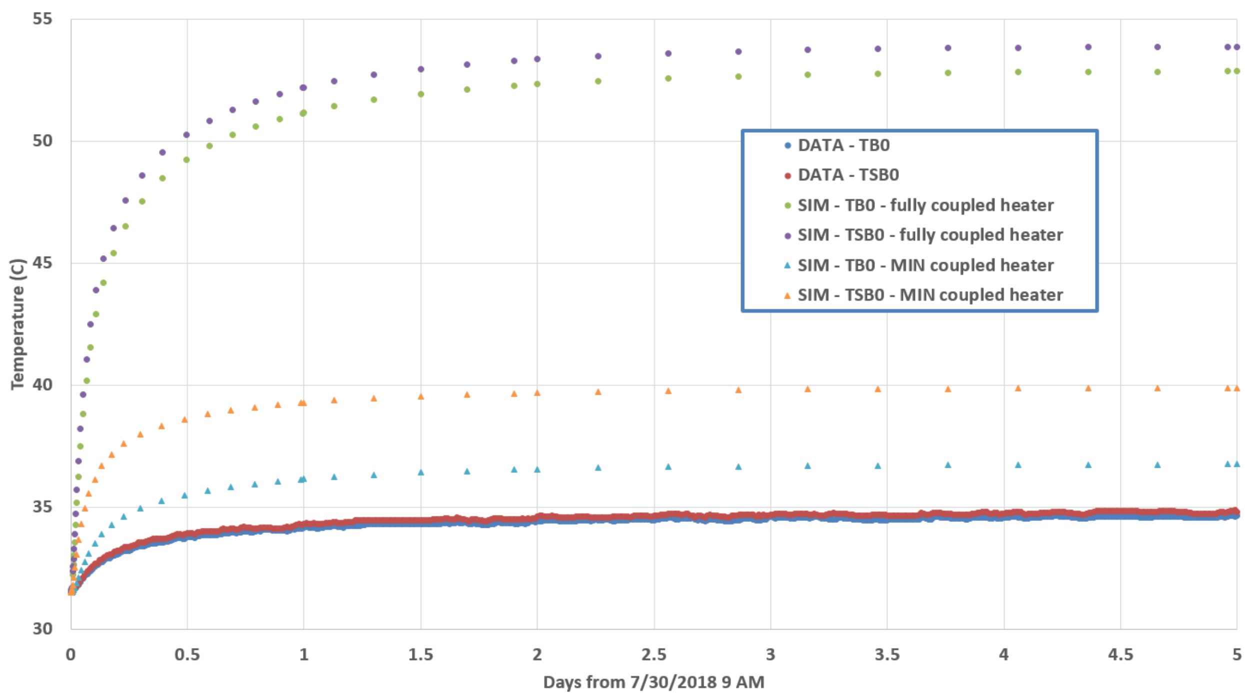

Figure 25 Temperature as a function of time at TB0 and TSB0, model vs data

Finally, we present simulations of the time dependent temperature response on nearby boreholes (TB and TBS, as shown on ***Figure 16***). The initial simulations of the experiment assumed full coupling between the heater and the borehole, resulting in the top points shown on ***Figure 25***. Simulations assuming full coupling clearly over predict the actual measured temperatures at monitoring locations TB0 and TSB0. A slice through the fully coupled heater simulation is shown in ***Figure 26***. There is no air gap between the heater and the borehole wall, thus for a fixed temperature (120°C), heat flow is maximized. Air has a low thermal conductivity, and radiative transport from the heater block is likely low at the 120°C temperature, as stainless steel is not optimized to generate radiative energy.

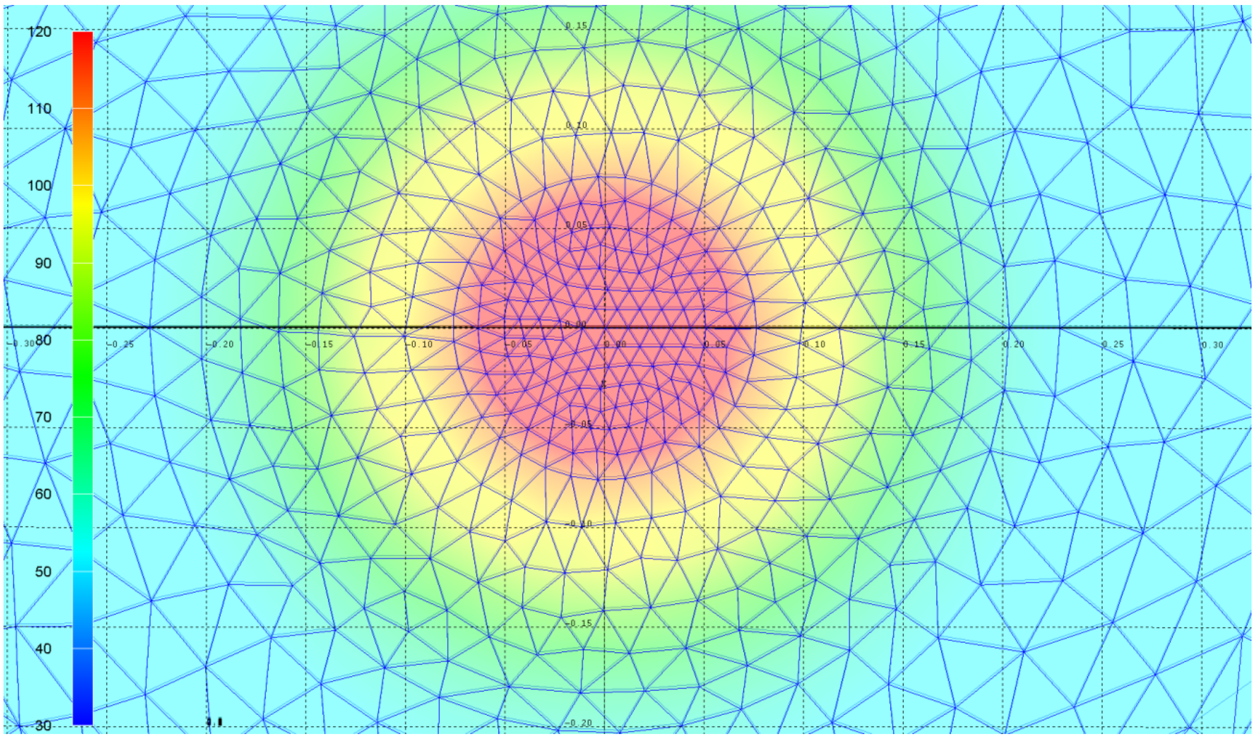

Figure 26. Fully coupled heater simulation.

Next, we added an air gap between the heater block and the borehole well to more accurately capture the experimental set-up, where the heater is sitting on the floor of the borehole with an air gap around most of the heater perimeter. As the coupled area is reduced, simulated temperatures in the surrounding boreholes begin to approach the data. The triangles shown on **Figure *25*** are for the least coupled case run for this report. The coupling for this case involves only 4 nodes along the radius of the heater block (**Figure *27***). This result has led to the consideration of infrared heating elements that can efficiently transmit energy through air.

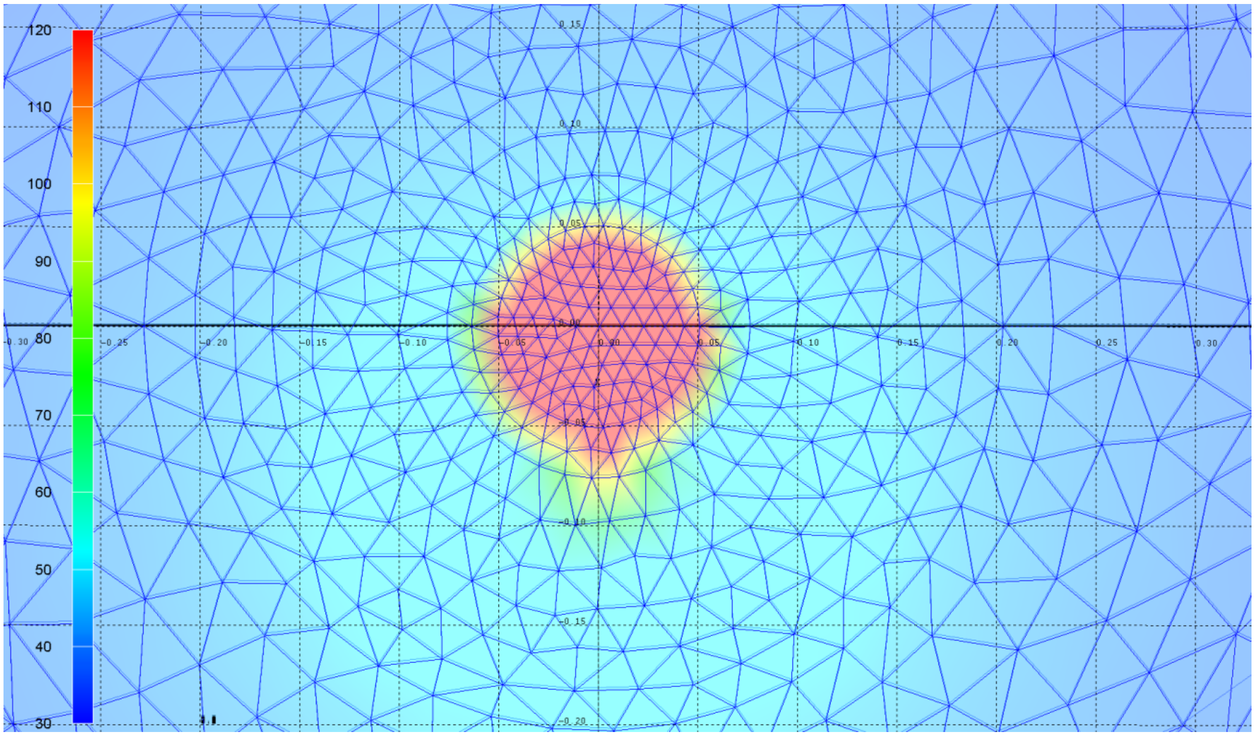

Figure 27 MIN coupled heater block

6. Conclusions and Recommendations

Shakedown testing of the field equipment for the thermal borehole testing at WIPP has proven to be extremely valuable for design and installation of a planned second phase in FY2019. Lessons learned will allow the team to move with much greater confidence and efficiency. Further, the integration of numerical analysis has allowed us to explore unexpected results such as lower than expected temperatures in surrounding boreholes. The lower than expected temperatures are likely caused by poor coupling of the heater block to the rock salt, leading us to adopt a new infrared approach for heating. Numerical analysis also confirmed a probable leak in the packer system, likely caused by bundling many wires through a 1" pass-through that was sealed with epoxy. The team is working to alleviate the leakage problem by using a different pass-through design and fewer wires behind the packer.

7. References

1. Carter, J.T., F. Hansen, R. Kehrman, and T. Hayes. 2011. A generic salt repository for disposal of waste from a spent nuclear fuel recycle facility. SRNL-RP-2011-00149 Rev. 0. Savannah River National Laboratory.
2. Callahan, G., D.C. Guerin, D.G. Levitt, D.L. Newell, B.A. Robinson, and L. Van Sambeek. 2012. Salt Repository Synthesis Data of Non-Delaware Basin and International Programs for the Storage/Disposal of Nuclear Waste. Los Alamos National Laboratory Report LCO-SDI-002.
3. DOE Carlsbad Field Office (DOE CBFO). 2012. A Management Proposal for Salt Defense Disposal Investigations (SDDI) for the Disposal of DOE-EM Managed Wastes. U.S. Department of Energy Carlsbad Field Office document.
4. Hansen, F.D. and C.D. Leigh. 2011. Salt disposal of heat-generating nuclear waste. Sandia National Laboratories Report SAND2011-0161.
5. Bradshaw, R.L., and W.C. McClain. 1971. Project Salt Vault: A Demonstration of Disposal of High Activity Solidified Wastes in Underground Salt Mines. ORNL-4555. Oak Ridge, TN: Oak Ridge National Laboratory.
6. Brewitz, W., and T. Rothfuchs. 2007. "Concepts and Technologies for Radioactive Waste Disposal in Rock Salt." Acta Montani stica Slovaca Ročník 12 (1) : 67–74.
7. Kühn, K. 1986. "Field Experiments in Salt Formations." Philosophical Transactions of the Royal Society of London A319: 157–61.
8. Krause, W.B., and P.F. Gnirk. 1981. Domal Salt Brine Migration Experiments at Avery Island, Louisiana. 81-04. Rapid City: RESPEC, Inc.
9. Matalucci, R.V. 1987. In Situ Testing at the Waste Isolation Pilot Plant. SAND87-2382. Albuquerque: Sandia National Laboratories.
10. Nowak, E.J., D.F. McTigue, and R. Beraun. 1988. Brine Inflow to WIPP Disposal Rooms: Data, Modeling, and Assessment. SAND88-0112. Albuquerque: Sandia National Laboratories.
11. Wicks, G.G. 2001. "U.S. Field Testing Programs and Results." Journal of Nuclear Materials 298, 78–85.
12. Hansen, F.D. and C.D. Leigh. 2011. Salt Disposal of Heat-Generating Nuclear Waste. SAND2011-0161.
13. Johnson, K.S., and S. Gonzales. 1978. Salt Deposits in the United States and Regional Geologic Characteristics Important for Storage of Radioactive Waste. Y/OWI/SUB-7414/1. Athens, GA: Earth Resources Associates.
14. Gellermann, Rainer. (2014). Lessons to be Learnt – The "ASSE" Case and the Challanges Concerning Disposal of Radioactive Waste.
15. Kuhlman, K. L., Malama, B. 2013. Brine Flow in Heated Geologic Salt. SAND2013-1944. Sandia National Laboratories. Albuquerque, NM.
16. Kuhlman, K.L., Mills, M.M., and Matteo, E.N., 2017. Consensus on Intermediate Scale Salt Field Test Design. Sandia National Laboratories, SFWD-SFWST-2017-000099, SAND1027 3179R, Albuquerque, NM.
17. Johnson, P.J., Bourret ,S.M., Boukhalfa, H., Caporuscio, F.A., Zyvoloski, G.A., Weaver, D.J., Otto, S., and Stauffer, P.H., 2017. Experiments and Modeling to Support Field Test

Design. Los Alamos National Laboratory, SFWD-SFWST-2017-000102, LA-UR-17-27759, Los Alamos, NM.
18. Kröhn, K.-P., Stührenberg, D., Jobmann, M., Heemann, U., Czaikowski, O., Wieczorek, K., Müller, C., Zhang, C.-L., Moog, H., Schirmer, S. and Friedenberg, L., 2017. Mechanical and Hydraulic Behavior of Compacting Crushed Salt Backfill at Low Porosities: Project REPOPERM – Phase 2. Gesellschaft für Anlagen- und Reaktorsicherheit (GRS) gGmbH, GRS-450. Braunschweig, Germany.
19. Stauffer, P.H., Jordan, A.B., Weaver, D.J., Caporuscio, F.A., Ten Cate, J.A., Boukhalfa, H., Robinson, B.A., Sassani, D.C., Kuhlman, K.L., Hardin, E.L., Sevougian, S.D., MacKinnon, R.J., Wu, Y., Daley, T.A., Freifeld, B.M., Cook, P.J., Rutqvist, J., and Birkholzer, J.T., 2015. Test proposal document for phased field thermal testing in salt. Los Alamos National Laboratory, FCRD-UFD-2015-000077, Los Alamos, NM.

8. Appendix A: Components Design and Specifications

List of Figures for Appendix A

Figure A- 1. Schematic representation of the heater cartridge heater used to build the block heater under in Phase 1. 47

Figure A- 2 Schematic representation of the Phase 1 block heater and a picture showing the actual heater block with the heater cartridge, supporting threaded rods and thermocouple wires mounted on the surface of the heater block. 49

Figure A- 3. Image showing the temperature controller J-CHEM Model 210. 50

Figure A- 4. Schematic representation of the packer system. 51

Figure A- 5. Packer pressure certification provided by the manufacturer 53

Figure A- 6. Figure showing the LVDT assembly mounted on a 1 in central pipe. 54

Figure A- 7. Detailed schematic diagram of the borehole deformation gauge. 55

Figure A- 8. Images showing the calibration of the Phase 1 borehole deformation gage. 56

Figure A- 9. Image of the Phase 1 DT722 relative humidity probe used to monitor RH and temperature of the gas circulated in the heated borehole. 58

Figure A- 10. DRIERITE cartridges used for Phase 1 moisture capture. 59

8.1. Heating Element Specifications

The heating element was manufactured by Watlow (**Figure A-** ***1***). The heating element selected was FIREROD Cartridge Heater with threaded fitting.

The technical details of the heating element are shown in **Figure A-** ***1***

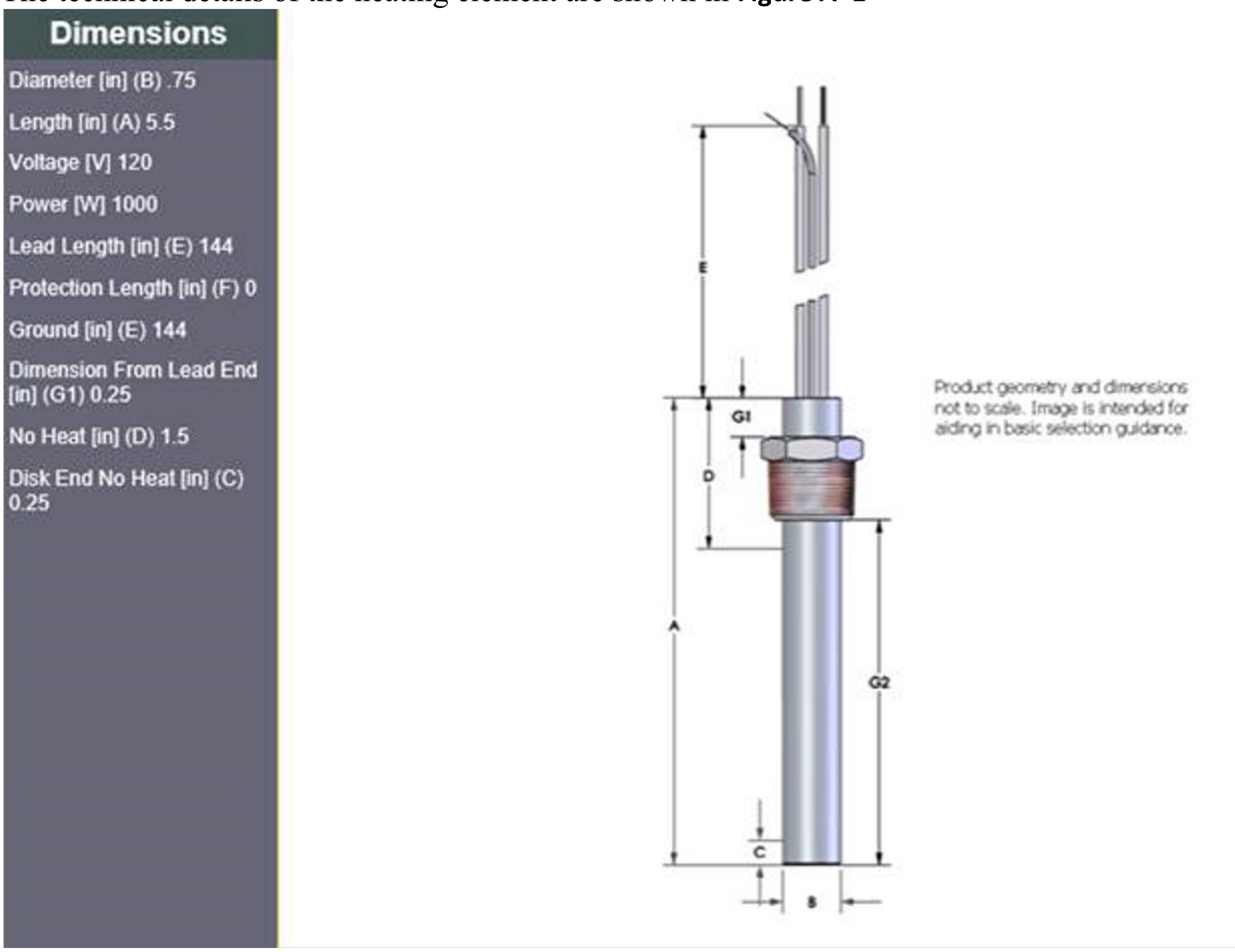

Figure A- 1. Schematic representation of the heater cartridge heater used to build the block heater under in Phase 1.

Additional details of the construction and performance of the heater can be found on Watlow website: *https://www.watlow.com/-/media/documents/catalogs/cartridge1-31.ashx*

8.2. Heating Block Specifications

The heating block used to construct the block heater was machined at a Los Alamos machining shop. The block material was 316 stainless steel. The heating block was machined in the form of a cylinder with a centralized hole sized to house the cartridge heater. A female NPT thread was added to the top part of the heater to secure the heater connection. Two pass-through holes 5/8" in diameter were drilled into the block heater to facilitate the insertion of threaded rods used to support the heater and centralize the LVDT system. An additional 3/8" in pass-through hole was drilled through the heater block to facilitate the passage to a Teflon sampling tube to borehole past the heater block. A picture of the actual heating block is shown in the **Figure A-** ***2***

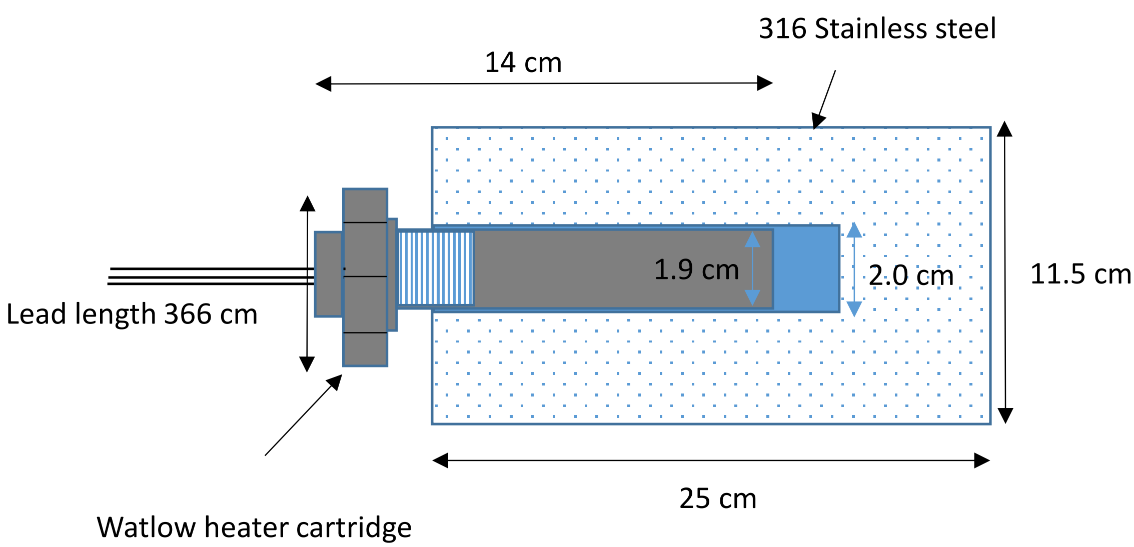

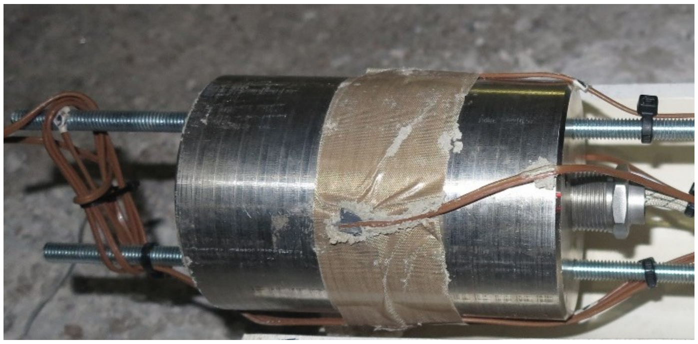

Figure A- 2 Schematic representation of the Phase 1 block heater and a picture showing the actual heater block with the heater cartridge, supporting threaded rods and thermocouple wires mounted on the surface of the heater block.

The dimensions of the heater block are:

Length: 5.5"

Diameter: 4.5"

Central cartridge hole length: 1/2"

Central cartridge diameter: 4.5"

Material: Stainless steel 316

8.3. Temperature Controller

The heating block temperature is controlled by a J-KEM scientific temperature controller model 210. The controller is equipped with a K-type thermocouple that attaches to the heating block and dial to set to desired temperature. A photograph of the model used in shown in **Figure A-** ***3***. This specific controller was selected because it is known to be reliable, safe, and has the ability to achieve temperatures within 0.1°C of the set point. Model 210 is a compact temperature controller that can power a heaters of up to 1200 watts of power. This specific model has the capacity to power heating blocks of up to 5 L in size. More information on the controller can be obtained from J-KEM scientific website: https://www.jkem.com/temperature-controllers/precision-controllers/model-210-controller

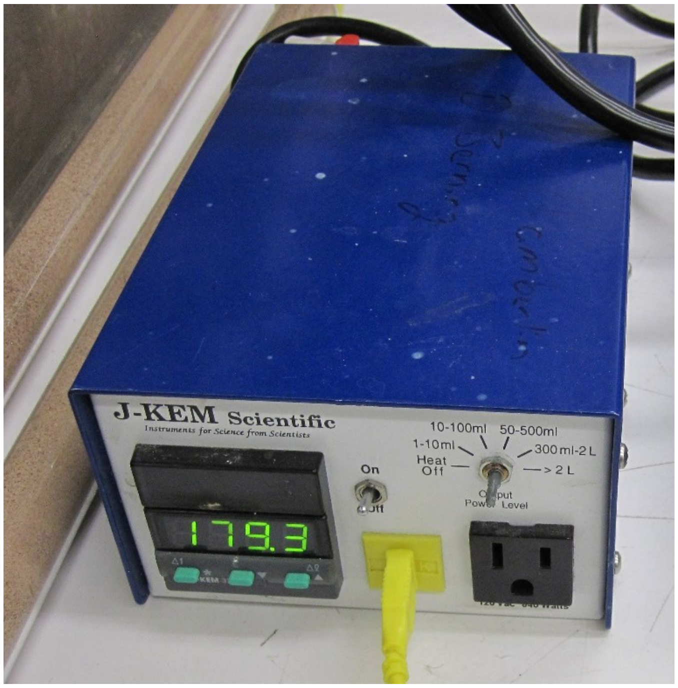

Figure A- 3. Image showing the temperature controller J-CHEM Model 210.

8.4. Packer Assembly Specifications

The packer used to isolate the heated borehole from the drift area was custom built by Aardvark Packers. The packer system designed to allow the isolation of the heated borehole from the drift area. The design of the packer included a set of pass-through tubes designed to access the isolated area of the borehole and allow the reading of the pressure behind the packer for gas permeability measurements. The details of drawing of the packer are shown in **Figure A- *4***. The large number of pass-through ports and miscommunications with the manufacturer resulted in several design issues that were not discovered until the unit was deployed underground at WIPP. Subsequent redesign and troubleshooting of the packer resolved most of the issues but it was less than ideal. Most of the issues were related to the discovery of leaks in fitting that connected the pass-through tubes to the packer metallic plates.

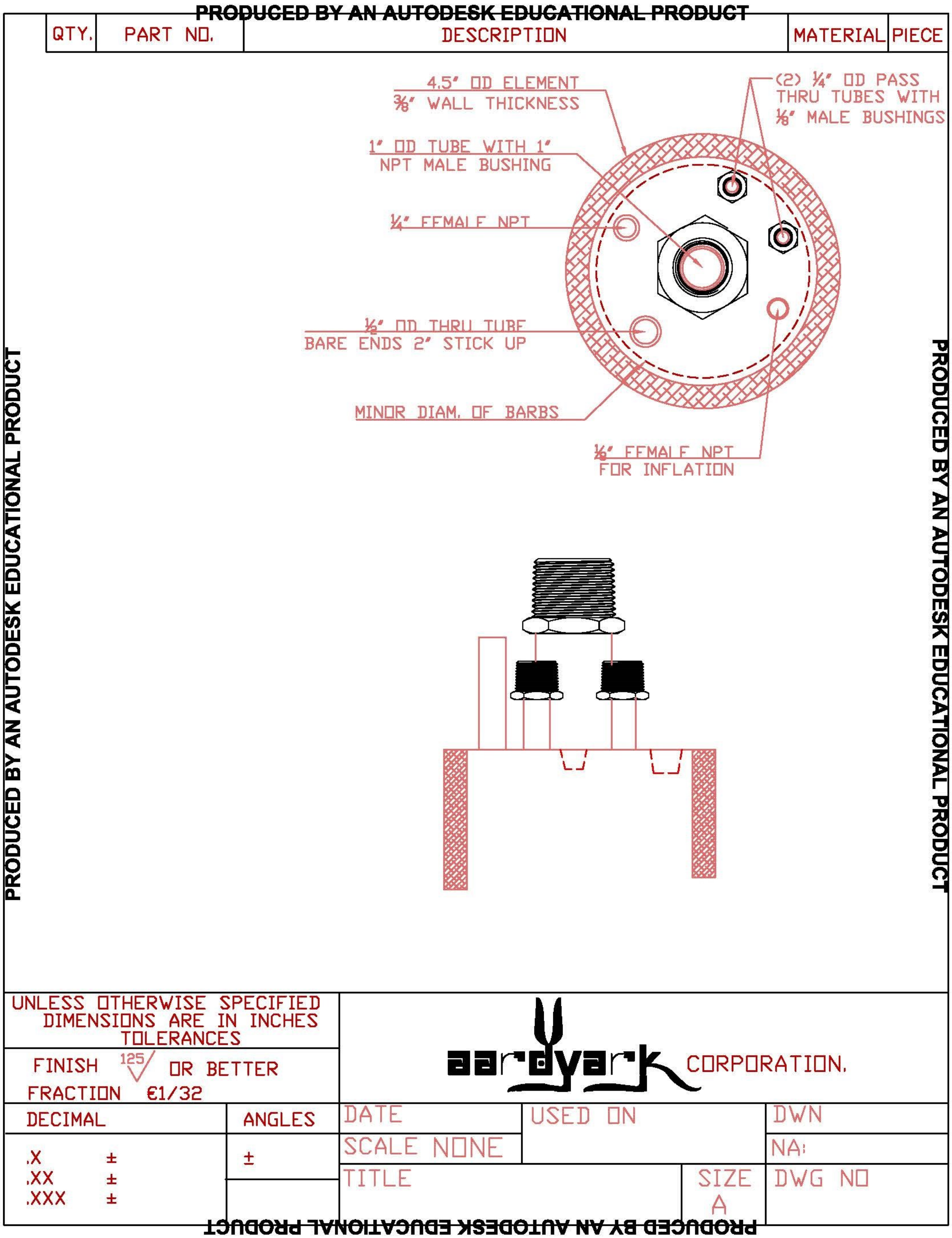

Figure A- 4. Schematic representation of the packer system.

The technical details of the packer assembly are as follows:

Diameter [in]: 4.5"

Overall Length [in]: 26"

3/8" wall thickness

Inflation port: 1/8" Female NPT

2 1/4" pass through tubes with Swagelok fittings

3/8" pass-through tube with female NPT

1" OD tube with 1" NPT female bushing

Maximum inflatable pressure unconfined: 15 PSI

Maximum inflatable pressure confined: 100 PSI

A picture of the packer system is shown in figure 7.

The pressure ratings of the packer are specified the pressure certification shown in **Figure A- 5**.

Aardvark PACKERS

Aardvark Packers Test Report

ITEM: 20448-7A	Quantity: 1
Part Number:	20448-7A
Date:	1/29/2018
Description:	Fixed end Packer: 4-1/2" x 20"
PSI UN-CONFINED	15 PSI
PSI (CONFINED)	100 PSI
Minutes Under pressure:	97 minutes
Test Facility:	Hydrostatic pressure test tank:
Notes:	Los Alamos Nat'l Labs. No Air/gas leaks noted during Inflation test.

Comments:

Packer was subjected to 2 tests. Un-Confined, under water with an inflation pressure of 15 psi. The packer was inflated with nitrogen and showed no leakage.

Stage II testing involved inflating the packer inside a 24" long PVC casing of 5" schedule 40. The packer was inflated to 100 psi and held pressure <2psi for a total of 97 minutes and held at 98 psi for the duration.

Stage II was also tested in the Hydrostatic Test Tank.

Aardvark Packers LLC
450 California Street
Grants Pass, OR 97526: 855-546-6488: sales@aardvarkpackers.com

Testing operator: [signature] Date: 1/29/2018

Figure A- 5. Packer pressure certification provided by the manufacturer

8.5. Borehole Deformation Gauge Specification

The borehole deformation gauge system was custom constructed by a machine shop in Albuquerque according to design specifications provided by Sandia National Laboratory staff. The gauge was designed to accurately measure changes in the radial dimension of a borehole in multiple directions. Four bow springs are used to centralize the gauge and deflect more or less with deformation of the borehole. Deflection of the bow springs causes one end of the assembly to move. Calculations based on a simplification of the bow springs' deflection with closure suggested that the movement of the sliding end will be linear over a range much larger than that anticipated in the field test. The movement of the sliding end was indeed found to be linear over the range of different diameters used during calibration. A picture of the gauge custom built for Phase 1 testing is shown in **Figure A- *6***.

Figure A- 6. Figure showing the LVDT assembly mounted on a 1 in central pipe.

The technical details of the LVDT system are shown in **Figure A-** *7*:

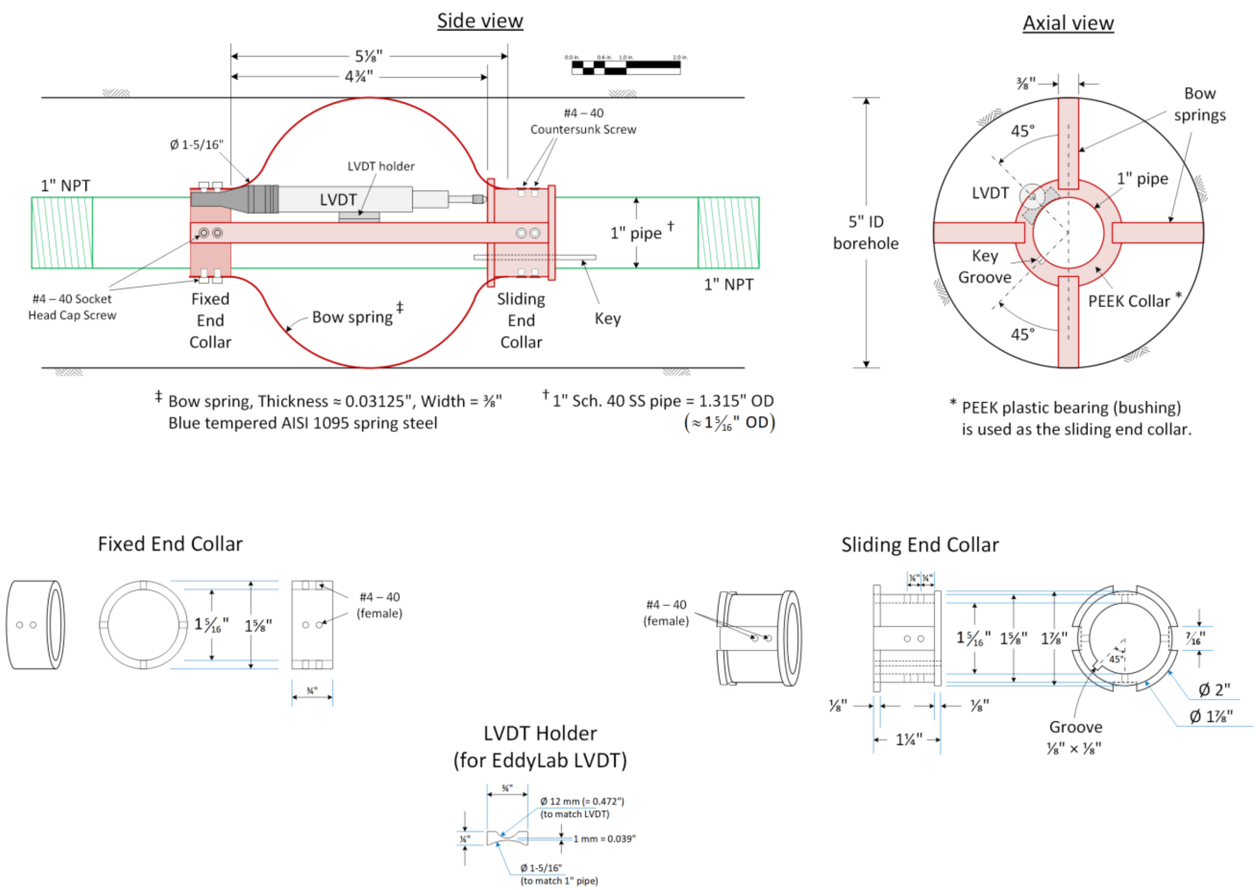

Figure A- 7. Detailed schematic diagram of the borehole deformation gauge.

LVDT Calibration was performed using a 0.010 inch (0.254 mm) thick × 3 inches (76.2 mm) wide × 18 inches (457 mm) long coiled strip of stainless steel shim material which was marked at various lengths corresponding to known diameters. The measurement of the movement of the sliding end collar is made using a linear variable differential transformer (LVDT) from eddylab GmbH with a measurement range of 5 mm. The picture in **Figure A- *8*** shows an image of the gauge inserted in one of the calibration cylinders of known diameter.

Figure A- 8. Images showing the calibration of the Phase 1 borehole deformation gage.

8.6. Brine Inflow Measurements

An experimental setup was constructed using off the shelf components to quantify brine release during the heater test. The setups consisted of a flow meter and flow controller, nitrogen flushing lines that allow dry nitrogen to be circulated through the heated borehole area to drive moisture released into the borehole to a measurement chamber equipped with a relative humidity probe, which continually monitors the RH. The gas leaving the measurement chamber is passed through two cartridges filled with a desiccant. The cartridges are weighted regularly to quantify the amount of water captured

The relative humidity probe used in this setup is a DT722 Rugged Industrial Relative Humidity and Temperature Transmitter - Duct Mount procured from Michell instruments (**Figure A- *9***). The probe measures relative humidity and temperature and transmits the data to a data-logger. The technical performance of the probe are:

Measurement Range (RH) 0-100% RH

Measurement Range (T) -40 to +150°C (-40 to +302°F)

Humidity <±2% RH (5-95% RH)

Temperature ±0.2°C (±0.36°F) typical

Stability - RH Sensor <±1% RH/year

Response Time <10 sec typical (for 90% of the step change)

Operating range 10 to 95% RH (non-condensing)

Housing Material Stainless Steel

Electrical Connections 5 pin, M12

More information can be obtained directly from the instrument's manufacturer website: http://www.michell.com/us/products/dt722.htm

Figure A- 9. Image of the Phase 1 DT722 relative humidity probe used to monitor RH and temperature of the gas circulated in the heated borehole.

The cartridges and desiccant were obtained from Drierite. The dryrite is a calcium sulfate desiccant. The part number of the cartridges is: L68NP303 Laboratory Gas Drying Unit with SS fittings. The field deployed canisters are shown in **Figure A- *10***. The specifications of the drying units as provided by the vendor are:

Construction: Column is molded polycarbonate. Desiccant supports and coil spring are stainless steel. Polycarbonate cap is fitted with o-ring gasket. DRIERITE is held firmly in place between felt filters.

Dimensions: 2 5/8" x 11 3/8"

Max working pressure: 90 psig

Desiccant: 1 1/4 Ib. 8 mesh Indicating DRIERITE

Water capacity: 50 grams

Recommended flow rate: 200 liters per hour

Pressure drop: <.01 psi at 200 lph

Figure A- 10. DRIERITE cartridges used for Phase 1 moisture capture.

An Omega gas flow meter model The FMA-LP1600A was used to control the flow rate of the nitrogen gas. The flow meter was fitted on the inlet port of the gas tubing that circulate the nitrogen gas in the heated borehole.

8.7.Data Acquisition and Logging

RH and temperature measurements were collected by connecting the thermocouple array, pressure transducers and RH probe directly to a Campbell Scientific, Inc. Measurement and Control Data-loggers, Model CR1000. The data-logger can perform measurements in ± 5000 mV or 4-20 mA, with measurement accuracy ± 0.12% reading. Other parameters such as the weight of the cartridges was, and other experimental notes were recorded in s scientific notebook, SDI-SN-0001, *Salt Defense Disposal Investigations General Scientific Notebook.* Data collected were disseminated to the staff working on the project in an electronic format through e-mail and other network file transfer.

9. Appendix B: Working Underground at WIPP

9.1. Qualifications and Training

Participants performing work under this test plan are required to read this test plan, associated technical procedures, and work control documents as applicable to the work. Site-specific training is provided by the WIPP site and scheduled through the TCO. To conduct physical work in the WIPP underground, WIPP General Employee Training and Underground Hazard Training is required. To operate compressed gas cylinders, Compressed Gas Training is required. At the start of each shift, a pre-job briefing is conducted with all affected staff to communicate the tasks, potential hazards, and mitigations of the work and work area. Required training specific to technical operating procedures is defined by the principle investigator for the activity.

9.2. Health and Safety

It is mandatory that all WIPP underground science program participants and personnel performing work associated with the science and testing activities in the WIPP underground and on the WIPP site abide by the NWP guidelines and requirements established in WP 02-EC.12, *Site Users and Tenants Guide for Organizations, Personnel, or Companies that Perform Work on U.S. Department of Energy Property or Rights-of-way on or Around the Waste Isolation Pilot Plant*, and the requirements of their home institutions or laboratories. The DOE-CBFO holds NWP accountable for safe operations at the WIPP and gives NWP authority to enforce safety rules and policies on all WIPP science participant organizations. As such, an Integrated Project Team Charter (DOE/CBFO-13-3515) was developed to define the processes, organizations, and interfaces necessary to conduct science and testing activities in the WIPP underground.

The health and safety hazards associated with this work are chemical, electrical, environmental, and thermal. The health and safety hazards are controlled and mitigated through TCO Work Control Documents and associated Job Hazard Analyses developed in accordance with SDI-SP-001, *Testing Work Authorization and Control*.

A safety document for the ERT system will be constructed based on existing LBNL procedures and documentation. The system uses between 50 and 250 volts depending on the conductivity of the formation. Electrical current is not anticipated to travel beyond the electrodes and is unlikely to impact power, grounding, communication, or other WIPP systems. Precautionary evaluations will be conducted prior to final emplacement and activation of the ERT system.

9.3. Permits and Authorizations

No special permits, licensing requirements, or special authorizations are required to conduct the scientific activity. Authorization to conduct work in the underground will be obtained through the world control process defined in DOE/CBFO-13-3515, *Science Testing Activities in* *the WIPP Underground – Integrated Project Team Charter*. Equipment not listed and labeled by a nationally recognized testing laboratory as defined by WP 23.IS0301, *NRTL Process*, must be approved by the Authority Having Jurisdiction before being used at the WIPP site.

The ERT data acquisition system will need to be evaluated by qualified WIPP electricians before it can be used for the experiment.